Bulletin of the Geological Society of Finland, Vol. 79, 2007, pp. 175–201

Sm-Nd data for mafic-ultramafic intrusions in the Svecofennian (1.88 Ga) Kotalahti Nickel Belt, Finland – implications for crustal contamination at the Archaean/Proterozoic boundary

Hannu V. Makkonen[1)]* and Hannu Huhma[2)]

[1)] *Geological Survey of Finland, P.O. Box 1237, FI-70211 Kuopio*

[2)] *Geological Survey of Finland, P.O. Box 96, FI-02151 Espoo*

Abstract

Sm-Nd data were determined for eight mafic-ultramafic intrusions from the Svecofennian (1.88 Ga) Kotalahti Nickel Belt, Finland. The intrusions represent both mineralized and barren types and are located at varying distances from the Archaean/Proterozoic boundary. The samples for the 23 Sm-Nd isotope analyses were taken mostly from the ultramafic differentiates. Results show a range in initial ε_{Nd} values at 1880 Ma from -2.4 to +2.0. No relationship can be found between the degree of Ni mineralization and initial ε_{Nd} values, while a correlation with the geological domain and country rocks is evident. The Majasaari and Törmälä intrusions, which have positive ε_{Nd} values, were emplaced within the Svecofennian domain in proximity to 1.92 Ga tonalitic gneisses, which have previously yielded initial ε_{Nd} values of ca. +3. In contrast, the Luusniemi intrusion, which has an ε_{Nd} value of -2.4 is situated close to exposed Archaean crust. Excluding two analyses from the Rytky intrusion, all data from the Koirus N, Koirus S, Kotalahti, Rytky and Kylmälahti intrusions, within error limits, fall in the range -0.7 ± 0.3. The results support the concept of contamination by Archaean material in proximity to the currently exposed craton margin. The composition of the proposed parental magma for the intrusions is close to EMORB, with initial ε_{Nd} values near +4.

Key words: intrusions, ultramafics, gabbros, nickel ores, geochemistry, Sm/Nd, magma contamination, tectonics, Proterozoic, Kotalahti, Finland

*Corresponding author email: hannu.makkonen@gtk.fi

1. Introduction

Most of the nickel-bearing Svecofennian (1.88 Ga) mafic-ultramafic intrusions in Finland are situated around the margins of the Central Finland Granitoid Complex, in the Kotalahti and Vammala Nickel Belts. The Kotalahti Nickel Belt also lies close to the Archaean/Proterozoic boundary (Fig. 1, Häkli, 1971; Gaál, 1972; Häkli et al., 1979; Mäkinen & Makkonen, 2004; Peltonen, 2005). The magmatism that produced the ore-bearing intrusions was broadly coeval with the Svecofennian orogeny and the emplacement of the magma took place during the maximum intensity of deformation and metamorphism (Mäkinen & Makkonen, 2004; Makkonen, 2005; Peltonen, 2005). It has been suggested that the composition of the parental magma was basaltic with a MgO content of about 12 wt.% (Peltonen, 1995a, 2005; Makkonen, 1996). Emplacement of magma was accompanied the gently dipping D_2 folding and thrusting event (Mäkinen & Makkonen, 2004; Makkonen, 2005), which was a response to convergence and thrusting of Svecofennian terranes over the Archaean cratonic foreland (Koistinen, 1981). During D_3 the subhorizontal $D_{1\text{-}2}$ structures were reoriented into steeper orientations (Mäkinen & Makkonen, 2004).

The mafic-ultramafic intrusions are commonly enclosed within regionally metamorphosed and migmatized Svecofennian turbiditic metasediments, which show various degrees of assimilation by the mafic magma. It has been proposed that this process of assimilation resulted in the formation of geochemically and mineralogically distinctive types of melt and mineral parageneses. According to Makkonen (1996) clinopyroxene-rich peridotites in the Juva area crystallized from uncontaminated magma (Vammala type, Mäkinen, 1987), while orthopyroxene-rich peridotites with intercumulus plagioclase (Kotalahti type, Mäkinen, 1987) reflect increased SiO_2 and Al_2O_3 in the magma, due to contamination by pelitic country rock. Similar conclusions were drawn by Makkonen et al. (2007) in a geochemical study of 11 intrusions in the Kotalahti Nickel Belt.

Sm-Nd isotopic studies indicate that felsic igneous rocks in the Svecofennian domain in Finland tend to have initial ε_{Nd} values from + 3 to -1 while corresponding values for mafic rocks, including mafic-ultramafic intrusions, range from + 3 to 0 (Huhma, 1986; Patchett & Kouvo, 1986; Makkonen, 1996). Rocks with distinctly positive initial values, including some of the mafic and ultramafic volcanics and the bulk of the 1.92 Ga crust within the Kotalahti Nickel Belt (Lahtinen & Huhma, 1997), suggest derivation from depleted mantle sources, without significant contributions from older LREE -enriched lithospheric material. In contrast, initial ε_{Nd} values close to zero obtained on some mafic-ultramafic rocks suggest heterogeneity in mantle sources or assimilation of crustal material.

For this study, samples were collected from eight intrusions within the Kotalahti Nickel Belt, representing both mineralized and barren intrusions, located at various distances from the Archaean/Proterozoic boundary (Fig. 1) and surrounded by different types of country rock. The purpose of the study is to compare the Sm-Nd isotope composition of mineralized and barren intrusions and discuss the role of crustal contamination.

2. Analytical methods

The chemical analyses were performed at the Geological Survey of Finland (GTK) Espoo laboratories. For whole rock analysis each sample was crushed in a Mn steel jaw crusher and pulverized in a tungsten carbide bowl before analysis by XRF (pressed powder pellets). Samples were also analysed for REE and other trace elements (HF-$HClO_4$ digestion, lithium metaborate - sodium perborate fusion; ICP-MS determination, Rautiainen et al., 1996).

For Sm-Nd studies samples were selected on the basis of the whole-rock and REE compositional data and the same powders were used for both chemical and isotopic analyses. The samples (150 – 200 mg) were dissolved in HF-HNO_3 using Savillex screw cap teflon beakers for 48 h. Mixed ^{149}Sm-^{150}Nd spike was added to the sample prior the dissolution. After careful evaporation of fluorides, the residue was dissolved in 6N HCl and a clear solution was achieved. Sm and Nd were separated in two stages using a conventional cation exchange procedure (7 ml of AG50Wx8 ion exchange resin in a bed of 12 cm length) and a modified version of the Teflon-HDEHP (hydrogen diethylhexyl phosphate) method developed by Richard et al. (1976). The measurements were made in a dynamic mode on a VG SECTOR 54 mass spectrometer using Ta-Re triple filaments. ^{143}Nd/^{144}Nd ratio is normalized to ^{146}Nd/^{144}Nd = 0.7219. The average value for the La Jolla standard was ^{143}Nd/^{144}Nd = 0.511850 ± 12 (1σ, n = 32). The Sm/Nd ratio of the spike has been calibrated against the Caltech mixed Sm/Nd standard (Wasserburg et al., 1981). Based on duplicated analyses, the error in ^{147}Sm/^{144}Nd is esti-

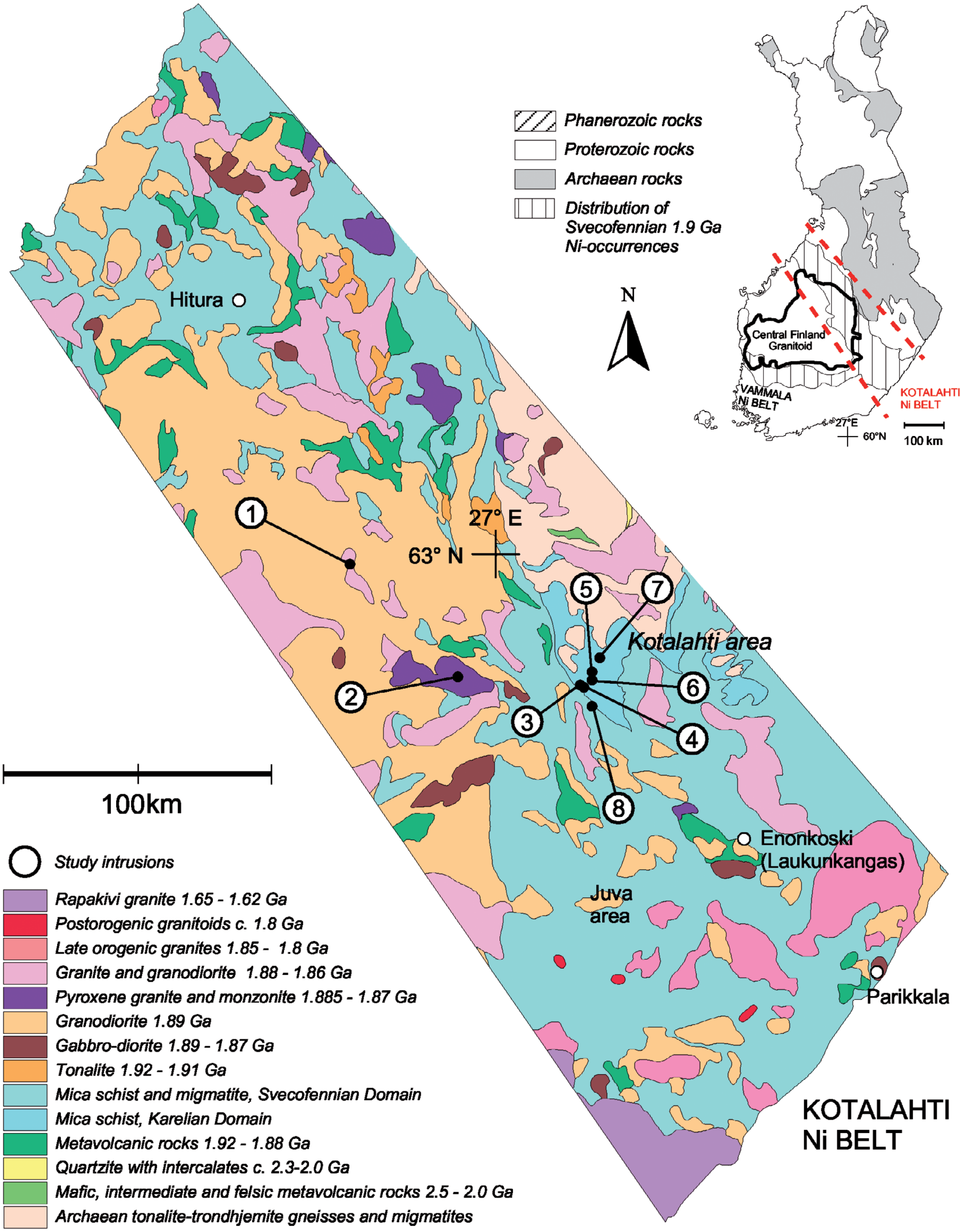

Fig. 1. Location and lithologies in the Kotalahti Nickel Belt in Finland. Studied intrusions indicated by the numbers: 1 = Majasaari, 2 = Törmälä, 3 = Kotalahti, 4 = Rytky, 5 = Koirus N, 6 = Koirus S, 7 = Luusniemi, 8 = Kylmälahti. Lithological maps simplified after Korsman et al. (1997). Hitura, Enonkoski and Parikkala Ni deposits and the Juva area also shown.

mated to be 0.4%. Initial $^{143}Nd/^{144}Nd$ ratios and ε_{Nd} values were calculated with the following parameters: $\lambda^{147}Sm = 6.54 \times 10^{-12}a^{-1}$, $^{147}Sm/^{144}Nd = 0.1966$ and $^{143}Nd/^{144}Nd = 0.51264$ for present CHUR. Depleted mantle model ages (T-DM) were calculated according to DePaolo (1981). Measurement on the rock standard BCR-1 provided the following values: Sm = 6.58 ppm, Nd = 28.8 ppm, $^{147}Sm/^{144}Nd = 0.1380$, $^{143}Nd/^{144}Nd = 0.51264 \pm 0.00002$. The blank measured during analyses was: 30 – 100 pg for Sm and 100 – 300 pg for Nd. The Isoplot-program by Ludwig (2001) has been used for data handling.

3. Description of the intrusions

The intrusions are classified according to the amount and composition of the sulfides found in each intrusion. The mineralized intrusions include Kotalahti, Rytky and Törmälä and barren ones Majasaari, Luusniemi and Kylmälahti. Koirus N and Koirus S are classified as intermediate types.

3.1. Majasaari

The Majasaari intrusion is located in the Viitasaari area, within the Central Finland Granitoid Complex (Fig. 1). Mafic-ultramafic rocks are generally rare in this area (Pipping, 1972; Nironen & Front, 1992), while remnants of upper Svecofennian supracrustal rocks are found locally (Kousa & Lundqvist, 2000); the Majasaari intrusion is surrounded by granitoids and mica gneisses.

On the basis of magnetic survey measurements, the Majasaari intrusion (Fig. 1, no 1) is apparently a roundish body 1 km in diameter. The SE contact of the intrusion is vertical, while on the opposite side the contact is dipping at about 45 degrees towards the W or NW. The central part of the intrusive body is mainly composed of norite and locally also of gabbronorite and olivine gabbronorite. Near the SE margin, olivine gabbronorite grades into plagioclase-bearing lherzolite. Plagioclase in the gabbroic rocks has a distinct cumulus form, while in lherzolite it is an intercumulus mineral. All rock types in the intrusion are well preserved and the corona bands (orthopyroxene-clinoamphibole-spinel) between plagioclase and olivine are thin, possibly reflecting a relatively shallow crystallization level (thicker coronas are common in Svecofennian intrusions associated with high-amphibolite or granulite facies rocks, cf. Tuisku & Makkonen, 1999). Sulfides (pyrrhotite, pentlandite, chalcopyrite) occur only sporadically and metallic copper is found in some samples (Makkonen et al., 2007).

Samples for the Sm-Nd study are from the olivine gabbronorite and plagioclase-bearing lherzolite at the SE margin of the intrusion.

3.2. Törmälä

The Törmälä intrusion (Fig. 1, no 2) is located in the high-grade Rautalampi area, which belongs into the accretionary arc complex of central and western Finland (Korsman et al., 1997). The area represents the transition zone between the Central Finland Granitoid Complex and the Savo schist belt, some 40 km west of the closest known exposures of the Archaean craton. The central part of the Törmälä area is a domal feature with gneissic tonalites (1.93 – 1.91 Ga) in the core, together with the mafic-ultramafic rocks. The tonalites, which are the oldest rocks in the area (Lahtinen, 1994; Pääjärvi, 2000), are structurally overlain by mica gneisses.

The Törmälä gabbro-peridotite intrusion has a surface area of about 50 x 150 m and the thickness of the body is up to 40 m and dips gently to NW. The contacts with the surrounding gneissic tonalites are strongly tectonized. The main rock types are olivine gabbronorite and plagioclase-bearing lherzolite, while coarse-grained gabbronorite and pyroxenite is present at the margins of the intrusion. The central part of the intrusive body is slightly more mafic (higher whole-rock Mg-number and higher Fo) than at the margins. Sulfides (pyrrhotite, pentlandite, chalcopyrite) occur in varying amounts, either as coarse-grained disseminations or breccias throughout the intrusion. The highest sulfide concentrations are found near the footwall contact. Estimated mineral resources are 0.12 Mt at 0.6 wt.% Ni, 0.3 wt.% Cu and 6.0

wt.% S (Makkonen et al., 2007).

Samples for the Sm-Nd study are from the olivine gabbronorite in the SE part of the intrusion.

All other sampled intrusions are located in the Kotalahti area.

3.3. Kotalahti

In the Kotalahti area, Archaean rocks are overlain by Palaeoproterozoic quartzites, limestones, carbonate rocks, sulfide-bearing black schists and diopside-banded amphibolites, structurally, if not stratigraphically overlain by amphibole feldspar gneisses, cordierite mica gneisses and mica gneisses. However, the D_2 thrusting has commonly disrupted the primary stratigraphy. Svecofennian thermal and tectonic activity was strong around the Archaean Kotalahti Dome, as indicated by the presence of allochthonous Archaean gneiss units and by the schollen-schlieren migmatites formed during D_2 (Mäkinen & Makkonen, 2004). Among the studied intrusions, Rytky and Kotalahti probably represent the deepest stratigraphical level, because they formed at the contact between the Archaean and Proterozoic rocks or within the Archaean rocks. On the other hand the Luusniemi intrusion is located closest to a larger area of the Archaean basement (Fig. 1).

The Kotalahti intrusion (Fig. 1, no 3) is a subvertical sheet with a length of approximately 1.3 km and a maximum width of 200 m. The southernmost intrusive body extends downwards to a depth of more than 1000 meters (Papunen, 2003). The wall rocks of the intrusion consist of Archaean gneisses. The U-Pb zircon age obtained for a gabbro in the Kotalahti intrusion is 1883 ± 6 Ma (Gaál, 1980).

The rock types range from olivine cumulates to olivine-enstatite cumulates, orthopyroxenites, poikilitic gabbros, ophitic gabbronorites, and diorites (Papunen, 2003). Among the peridotitic rocks, coarse-grained lherzolite is found in the stratigraphic footwall and is overlain by medium-grained lherzolite (Mäkinen & Makkonen, 2004). Disseminated sulfides are common in ultramafic rocks and poikilitic gabbros whereas ophitic gabbros and diorites are almost barren. Breccia-type sulfides occur as irregular masses, commonly along the contacts in the thinner central part of the intrusion. A separate massive offset, called the Jussi ore body, is present as a subvertical slab in the black-schist and calc-silicate wall rock some 150 m east of the main ore body (Papunen, 2003). The total production at Kotalahti during 1959 – 1987 was 12.3 Mt at 0.7 % Ni and 0.3 % Cu (Puustinen et al., 1995).

Samples for the Sm-Nd study are from the coarse-grained lherzolite, medium-grained lherzolite and coarse-grained websterite in the northern part of the intrusion (Mertakoski).

3.4. Rytky

The surface section (0.5 x 1 km) of the Rytky intrusion (Fig. 1, no 4) comprises two blocks separated by Proterozoic supracrustal rocks and Archaean tonalite gneisses. The SE block is mainly surrounded by Archaean rocks and the NW block by Proterozoic rocks. The intrusion was originally funnel-shaped and layered. A minor part of the intrusion is represented by sills located below the main intrusion within the Archaean tonalite gneiss. Fragments of the intrusion were incorporated into the surrounding gneisses during D_2 overthusting. During D_3 the magmatic layering was folded into a subvertical orientation (Mäkinen & Makkonen, 2004).

On the basis of the three separate intrusive phases recognized, the rock types can be grouped as follows, beginning from the earliest phase: 1) coarse grained lherzolites and websterites/melagabbros, 2) medium-grained lherzolites, websterites and gabbronorites and 3) subophitic gabbros (Mäkinen & Makkonen, 2004).

Sulfides (pyrrhotite, pentlandite, chalcopyrite) are most abundant in the coarse-grained lherzolites and websterites/melagabbros, forming matrix ore. Sulfide disseminations occur in the medium-grained lherzolites and websterites. In places, narrow massive ore layers are present. Indicated mineral resources are 1.54 Mt at 0.71 % Ni, 0.29 % Cu and 4.45 % S (Finn Nickel Ltd press release, February 2007).

Samples for the Sm-Nd study are from coarse- and medium-grained lherzolite, coarse-grained websterite, melagabbro, websterite and olivine gabbronorite.

3.5. Koirus N

Two large intrusions occur in the Lake Koirusvesi area and according to their geographical position, they have been named Koirus N and Koirus S intrusions. The Koirus N intrusion (Fig 1, no 5) has a surface area of 0.5 – 1.0 x 2.5 km. According to the magnetic interpretation the magnetized units within the intrusion extend downwards to a depth of 400 m and dip steeply. Intrusion contacts have not been intersected but mica gneisses occur in outcrop in the immediate surroundings. The main rock type in the intrusion is norite with local gabbronorite and interlayers of websterite. Two serpentinite bodies, up to 200 m wide, have been found in the central part of the intrusion. An olivine websterite layer, more than 50 m thick was intersected at a depth of 200 – 300 m. Minor sulfide disseminations occur in norite (Ni $\leq$ 0.3 wt.%) but no nickel mineralization has been found within the intrusion.

Samples for the Sm-Nd study are from one of the serpentinite bodies and from the olivine websterite.

3.6. Koirus S

The Koirus S intrusion (Fig.1, no 6) has a somewahat circular surface section about 1 km in diameter. It is enclosed by mica gneisses and composed mainly of gabbroic rocks – gabbronorite and norite – with small amounts of hornblende gabbro and cummingtonite gabbro. Ultramafic rocks are present in the central part of intrusion, where they form a dunite-peridotite unit up to 100 m in thickness. Peridotite is mainly lherzolitic in mineral composition (minor wehrlite). Websterite layers are common within and near the peridotite. The stratigraphic footwall of the ultramafic unit is towards the SE, based on the whole rock and mineral chemistry (Makkonen & Ekdahl, 1984). Sulfides occur as weak to moderate dissemination in the peridotite-dunite unit, but the nickel content is low, usually less than 0.4 wt.%.

Samples for the Sm-Nd study are from the lherzolite in the NE end of the ultramafic unit.

3.7. Luusniemi

The Luusniemi intrusion (Fig. 1, no 7) is composed of gabbro and peridotite-pyroxenite units, which have been juxtaposed tectonically. At the present erosion level, the maximum dimension of the gabbro unit is about 5 km and that of the ultramafic unit nearly 1 km. The ultramafic unit is cone-shaped with the hanging wall contacts dipping about 45 degrees. The surrounding rocks are mica gneisses and granitoids. Granitoids are also known to intersect the ultramafic unit. The main minerals in the gabbroic rocks are plagioclase and clinoamphibole. The rock types in the ultramafic unit include partly serpentinized lherzolites, clinopyroxene dominated olivine websterites and websterites containing locally abundant magnetite. Gabbroic rocks are only locally present. A weak magmatic lamination is evident in the peridotites. Some olivine grains are heavily corroded and in places magmatic deformation lamellae are visible in olivine. These features suggest that olivine has been transported and that intrusion took place in several phases. Sulfides are very rare in the Luusniemi intrusion and they have been oxidised to magnetite in the NW part of the intrusion (Makkonen et al., 2007).

Samples for the Sm-Nd study are from the lherzolite in the southern part of the ultramafic unit.

3.8. Kylmälahti

The Kylmälahti intrusion (Fig. 1, no 8) is a narrow (50 m) N-S trending, vertical body surrounded by mica gneiss. It is composed of homogeneous but strongly sheared and altered wehrlitic peridotite. Metapyroxenite or hornblendite is found locally along intrusion margins. Sulfide disseminations (pyrrhotite, chalcopyrite, rare pentlandite) are common in peridotite, but are relatively poor in nickel and copper (Makkonen et al., 2007).

Samples for the Sm-Nd study are from the peridotite.

4. Geochemistry of the intrusions

Whole rock data for the studied samples are given in Table 1. It should be noted that the samples mostly represent the *ultramafic* differentiates for each intrusion, gabbroic samples having only been included from the Majasaari, Törmälä and Rytky intrusions. More geochemical data for the Kotalahti intrusion can be found in Papunen & Koskinen (1985) and for the other intrusions in Forss et al. (1999), Makkonen & Mäkinen (2003), Makkonen et al. (2003), Mäkinen & Makkonen (2004) and Makkonen et al. (2007).

The parental magma for the Svecofennian intrusions has been shown to be of basaltic composition, but different crystallization trends have produced a wide variety of cumulate rocks (Mäkinen, 1987; Peltonen, 1995a; Makkonen, 1996; Peltonen, 2005; Lamberg, 2005). The CMA plot (Fig. 2) reveals the principal geochemical differences between the intrusions. In Rytky, Koirus N, Majasaari and for the most part of the, Kotalahti intrusion, the principal cumulus mineral after olivine was orthopyroxene, while in Luusniemi and Kylmälahti it was clinopyroxene. Koirus S and Törmälä represent an intermediate trend. Most of the mineralized intrusions in the Kotalahti Nickel Belt have fractionation trends dominated by orthopyroxene and plagioclase , whereas barren intrusions have clinopyroxene-dominated trends (Makkonen & Mäkinen, 2003; Makkonen et al., 2007). These features are also shown by the samples of this study, although the small number of samples makes it difficult to define clear trends. The different fractionation trends have been attributed to an increase of SiO_2 in the magma during assimilation of country rock, which promotes the crystallization of orthopyroxene (Haughton et al., 1974). The assimilation also increases the Al_2O_3/CaO ratio in magma, which in turn favours the crystallization of plagioclase instead of clinopyroxene.

The intrusions display a relatively wide range in incompatible element concentrations for ultramafic rocks (Table 1). For example, Zr concentrations in Rytky range between 15 – 73 ppm (Fig. 3). High Zr abundances are also found in Koirus S and Majasaari, while the Zr content in Luusniemi is markedly lower than in the other intrusions. An overall positive correlation exists between Zr and magmatic differentiation as the relative amount of the intercumulus liquid increases. However, the wide range suggests that some other processes have also affected the observed values.

The abundance of REE correlate generally with the P_2O_5 content, as was also found for the intrusions in the nearby Juva area. High REE contents are associated with high P_2O_5 and in some peridotites the whole rock REE content is effectively equivalent to the REE present in apatite (Makkonen, 1996). The positive correlation between REE and P_2O_5 contents possibly reflects the controlling influence of the proportion of interstitial liquid on the concentrations of incompatible elements. Chondrite-normalized REE diagrams are shown in Fig. 4. The intrusions in the Kotalahti area are shown separately for the Majasaari and Törmälä intrusions. Also Kotalahti and Rytky, which occur close to each other (1 km), are shown on separate diagrams. The Kotalahti and Rytky intrusions differ with respect to their REE contents, which is probably due to the higher proportion of intercumulus liquid in the Rytky samples (cf. Fig. 3). The Kotalahti, Rytky and Koirus intrusions have sloping LREE trends, while those in Majasaari,Törmälä, Luusniemi and Kylmälahti are more flat. The flattest trends are observed in the barren Kylmälahti and Luusniemi intrusions, while conversely, the steepest trend is found in the mineralized Rytky intrusion; the mineralized Törmälä intrusion on the other hand, does not display a distinct sloping LREE trend.

5. Composition of the magma

It has been proposed that the parental magma of the Svecofennian nickel-bearing intrusions is a tholeiitic basalt with an MgO content ca 12 wt.% and trace element contents typical for arc tholeiites (Peltonen, 1995b) or for MORBs (Makkonen, 1996). Metabasalts consistent with the latter alternative can be found for example in the Rantasalmi and Enonkoski

Table 1. Whole-rock analytical data of the studied samples (Rytky and Kotalahti from Mäkinen & Makkonen, 2004).

Sample	1	2	3	4	5	6	7	8	9	10	11
Intrusion (no)	Majasaari (1)*	Majasaari (1)	Törmälä (2)	Törmälä (2)	Kotalahti (3)	Kotalahti (3)	Kotalahti (3)	Rytky (4)	Rytky (4)	Rytky (4)	Rytky (4)
Rock type	Plag-bearing lherzolite	Olivine gabbronorite	Olivine gabbronorite	Olivine gabbronorite	Lherzolite coarse-gr	Lherzolite, medium-gr	Websterite coarse-gr	Lherzolite coarse-gr	Lherzolite medium-gr	Melagabbro	Lherzolite coarse-gr
Country rock	Granitoids, mica gneiss	Granitoids, mica gneiss	Tonalite (1.93-1.91 Ga)	Tonalite (1.93-1.91 Ga)	Archaean gneiss, craton margin seq.	Archaean gneiss, craton margin seq.	Archaean gneiss, craton margin seq.	Archaean gneiss, craton margin seq.	Archaean gneiss, craton margin seq.	Archaean gneiss, craton margin seq.	Archaean gneiss, craton margin seq.
Ore formation	barren	barren	ore	ore	ore	ore	ore	ore	ore	ore	ore
SiO_2 (wt.%)	37.35	46.73	41.40	45.10	43.16	39.68	48.37	31.56	40.27	45.72	41.85
TiO_2	0.34	0.64	0.25	0.35	0.21	0.25	0.25	0.32	0.20	0.81	0.60
$Al2O_3$	6.13	20.09	9.96	7.62	4.07	4.42	5.81	4.43	4.41	9.23	7.11
FeOT	12.01	7.31	11.70	9.90	11.07	12.30	11.05	24.47	12.77	8.81	9.57
MnO	0.16	0.11	0.18	0.17	0.16	0.17	0.17	0.15	0.16	0.15	0.14
MgO	29.26	9.67	22.90	21.60	28.06	29.02	23.97	18.64	27.55	19.34	26.15
CaO	3.19	9.64	6.39	10.20	2.21	4.96	3.76	3.50	3.12	5.85	4.21
Na_2O	0.40	2.62	0.96	0.81	0.24	0.32	0.34	0.35	0.54	0.71	1.00
K_2O	0.13	0.27	0.17	0.20	0.33	0.07	0.12	0.35	0.29	1.17	0.59
P_2O_5	0.07	0.10	0.05	0.05	0.05	0.03	0.02	0.12	0.06	0.23	0.24
Total	89.04	97.18	93.96	96.00	89.56	91.22	93.86	83.89	89.37	92.02	91.46
MDI[1)]	21.90	34.27	26.12	23.84	20.53	19.41	17.81	44.38	26.67	28.14	26.83
Mg-number[2)]	0.81	0.70	0.78	0.80	0.82	0.81	0.79	0.58	0.79	0.80	0.83
Cl (ppm)	1033	78	1020	260	587	1875	64	223	871	161	774
Ba	63	104	71	82	88	51	52	143	164	189	335
Rb	6	11	8	7	11	2	5	12	9	36	14
Sr	92	401	180	111	47	91	71	138	110	135	546
Y	13	7	7	9	4	6	5	8	6	13	10
Zr	24	39	18	20	17	13	11	36	21	65	56
Nb	2	1	1	2	3	0	0	4	1	6	7
Th	<0.5	<0.5	0.25	0.25	<0.5	<0.5	<0.5	0.8	1	1.24	1.05
Pb	12	11	10	16	12	21	14	12	20	10	16
Ga	7	20	12	9	9	12	8	6	13	20	14
Zn	102	65	97	76	87	121	82	70	118	91	100
Cu	79	33	82	103	711	739	1101	4939	978	96	47
Ni	1154	303	407	330	2382	2511	2995	13080	3565	757	1535
S	637	470	890	1190	6465	10260	12350	8166	1597	20	1411
V	95	103	120	231	63	96	139	67	63	135	90
Cr	2968	210	1972	2255	1625	970	3281	362	1860	1730	638
Sc	8	19	17	42	13	20	31	9	12	25	9
U	<0.2	<0.2	0.1	0.1	0.42	<0.2	<0.2	0.42	0.6	0.65	0.41
La	2.79	4.37	2.45	2.65	3.3	2.31	1.65	11.3	4.99	18.2	16
Ce	6.36	11	4.77	5.03	7.18	5.61	3.58	25.3	11.4	43.7	37
Pr	0.81	1.54	0.63	0.71	0.8	0.83	0.44	3.03	1.56	5.53	4.52
Nd	4.28	7.04	2.8	3.2	3.84	3.83	2.24	11.7	5.94	21.3	17.2
Sm	0.96	1.97	0.76	0.94	0.66	1.05	0.63	1.97	1.31	3.73	2.88
Eu	0.32	0.79	0.35	0.35	0.19	0.33	0.16	0.59	0.37	1.09	0.78
Gd	1.11	2.25	0.94	1.34	0.91	1.07	0.7	1.98	1.21	3.96	2.94
Tb	0.2	0.35	0.16	0.25	0.12	0.19	0.12	0.27	0.17	0.48	0.35
Dy	1.25	2.17	1.15	1.57	0.63	0.96	0.82	1.42	0.84	2.55	1.68
Ho	0.24	0.43	0.23	0.33	0.13	0.24	0.15	0.29	0.22	0.45	0.33
Er	0.64	1.09	0.68	0.92	0.43	0.65	0.52	0.75	0.52	1.24	0.8
Tm	0.1	0.17	0.11	0.14	<0.1	<0.1	<0.1	0.13	<0.1	0.16	0.12
Yb	0.66	1.05	0.61	0.84	0.5	0.58	0.57	0.76	0.63	1.05	0.77
Lu	0.1	0.18	<0.1	0.13	<0.1	<0.1	<0.1	0.11	<0.1	0.16	0.11

[*)] Intrusion numbers (1-8) as in Fig. 1.
[1)] MDI = modified differentiation index (Gruenewaldt, 1973)
[2)] Mg-number = MgO/(MgO+FeOT) mol.%.
Yttrium (detection limit 0.1 ppm), Th (0.5 ppm) and U (0.2 ppm) by ICP-MS, other trace elements by XRF with the following detection limits: Sulfur ca. 100 ppm, Cl ca. 60 ppm; Sc, V, Cr,
Pb ca. 30 ppm; Ni, Cu, Zn, Ga, Ba ca. 20 ppm; Rb, Sr, Zr, Nb ca. 10 ppm.

Table 1. cont. Whole-rock analytical data of the studied samples (Rytky and Kotalahti from Mäkinen & Makkonen, 2004).

12	13	14	15	16	17	18	19	20	21	22	23
Rytky (4)	Rytky (4)	Rytky (4)	Rytky (4)	Koirus N (5)	Koirus N (5)	Koirus S (6)	Koirus S (6)	Luusniemi (7)	Luusniemi (7)	Kylmälahti (8)	Kylmälahti (8)
Melagabbro	Websterite	Websterite	Olivine gabbronorite	Olivine websterite	Serpentinite	Lherzolite	Lherzolite	Lherzolite	Lherzolite	Metaperidotite	Metaperidotite
Archaean gneiss, craton margin seq.	Archaean gneiss, craton margin seq.	Archaean gneiss, craton margin seq.	Archaean gneiss, craton margin seq.	Mica gneiss	Mica gneiss	Mica gneiss	Mica gneiss	Granitoids, Archaean gneiss	Granitoids, Archaean gneiss	Mica gneiss	Mica gneiss
ore	ore	ore	ore	interm	interm	interm	interm	barren	barren	barren	barren
49.66	41.92	49.52	50.16	50.80	36.70	41.10	37.90	46.10	40.90	42.20	43.30
0.72	0.25	0.51	0.36	0.36	0.26	0.59	0.41	0.34	0.26	0.40	0.49
11.44	4.62	8.44	9.70	5.50	3.97	5.17	4.61	2.93	1.91	3.77	4.72
7.79	10.40	8.98	8.52	10.62	13.05	11.16	12.96	10.98	15.12	12.96	13.68
0.14	0.16	0.16	0.16	0.19	0.18	0.16	0.17	0.19	0.26	0.19	0.14
15.32	28.78	22.18	21.19	26.00	30.30	24.50	26.40	17.50	23.00	20.70	20.70
6.81	4.45	4.98	5.45	2.96	1.67	6.53	5.34	15.00	9.97	10.30	9.14
2.09	0.32	0.78	0.95	0.48	0.24	0.48	0.50	0.33	0.11	0.36	0.46
0.90	0.11	0.23	0.15	0.16	0.15	0.46	0.26	0.13	0.08	0.15	0.18
0.31	0.04	0.05	0.03	0.04	0.10	0.12	0.11	0.02	0.01	0.03	0.03
95.18	91.05	95.83	96.67	97.11	86.62	90.27	88.66	93.52	91.62	91.06	92.84
36.74	19.79	21.85	21.90	20.93	23.88	25.27	25.21	27.22	28.70	26.10	27.10
0.78	0.83	0.81	0.82	0.81	0.81	0.80	0.78	0.74	0.73	0.74	0.73
246	1848	85	35	90	1540	823	1380	177	432	531	119
343	72	108	81	83	72	269	153	50	35	41	54
19	3	8	3	8	4	15	6	5	6	8	4
832	129	137	157	88	141	178	197	89	43	36	44
15	6	10	7	6	5	12	8	6	5	8	9
73	15	31	18	20	22	42	34	12	5	23	27
6	1	2	0	3	1	8	4	1	0	2	0
1.75	<0.5	<0.5	<0.5	0.25	0.25	0.56	0.25	0.25	0.25	0.25	0.25
19	11	13	11	12	14	15	18	13	12	16	15
17	10	15	14	9	9	12	6	4	10	6	7
104	78	79	70	101	119	115	114	64	94	76	63
45	161	82	70	28	36	51	490	110	216	628	612
509	1269	645	590	281	528	391	1640	140	257	546	437
1029	158	94	870	610	892	1380	7090	925	1260	7550	7140
123	108	161	159	203	94	129	115	242	190	237	262
1367	2830	3331	2927	2260	848	2120	2390	968	751	1560	1210
23	21	32	36	26	10	23	20	75	58	54	56
0.71	<0.2	<0.2	<0.2	0.1	0.1	0.23	0.21	0.1	0.1	0.1	0.1
23.9	2.93	4.19	2.68	3.11	6.05	8.12	6.59	2.88	2.67	1.81	3.31
53.9	6.67	9.59	6.03	5.4	9.6	20.3	14.1	6.27	3.58	4.32	5.84
6.54	0.89	1.18	0.83	0.75	1.21	2.87	1.95	0.94	0.6	0.67	0.85
25.9	3.84	5.58	3.88	3.17	5.38	12.7	8.56	4.97	3.35	3.39	4.27
4.28	0.86	1.2	0.89	0.71	1.02	2.72	1.7	1.24	0.98	0.88	1.11
1.25	0.28	0.42	0.27	0.25	0.32	0.83	0.59	0.41	0.29	0.34	0.44
4.11	0.9	1.59	1.17	0.86	1.05	2.53	1.79	1.45	1.08	1.27	1.63
0.53	0.16	0.24	0.2	0.13	0.15	0.39	0.25	0.21	0.16	0.21	0.29
2.76	0.87	1.46	1.22	0.91	0.87	2.19	1.28	1.15	0.85	1.38	1.63
0.54	0.19	0.33	0.26	0.18	0.18	0.4	0.28	0.21	0.18	0.28	0.35
1.28	0.52	0.97	0.66	0.55	0.5	1.14	0.73	0.56	0.41	0.86	0.99
0.19	0.1	0.14	0.12	<0.1	<0.1	0.16	<0.1	<0.1	<0.1	<0.1	0.13
1.19	0.58	0.94	0.77	0.59	0.46	0.96	0.68	0.52	0.38	0.7	0.82
0.21	<0.1	0.16	0.1	<0.1	<0.1	0.13	<0.1	<0.1	<0.1	<0.1	0.11

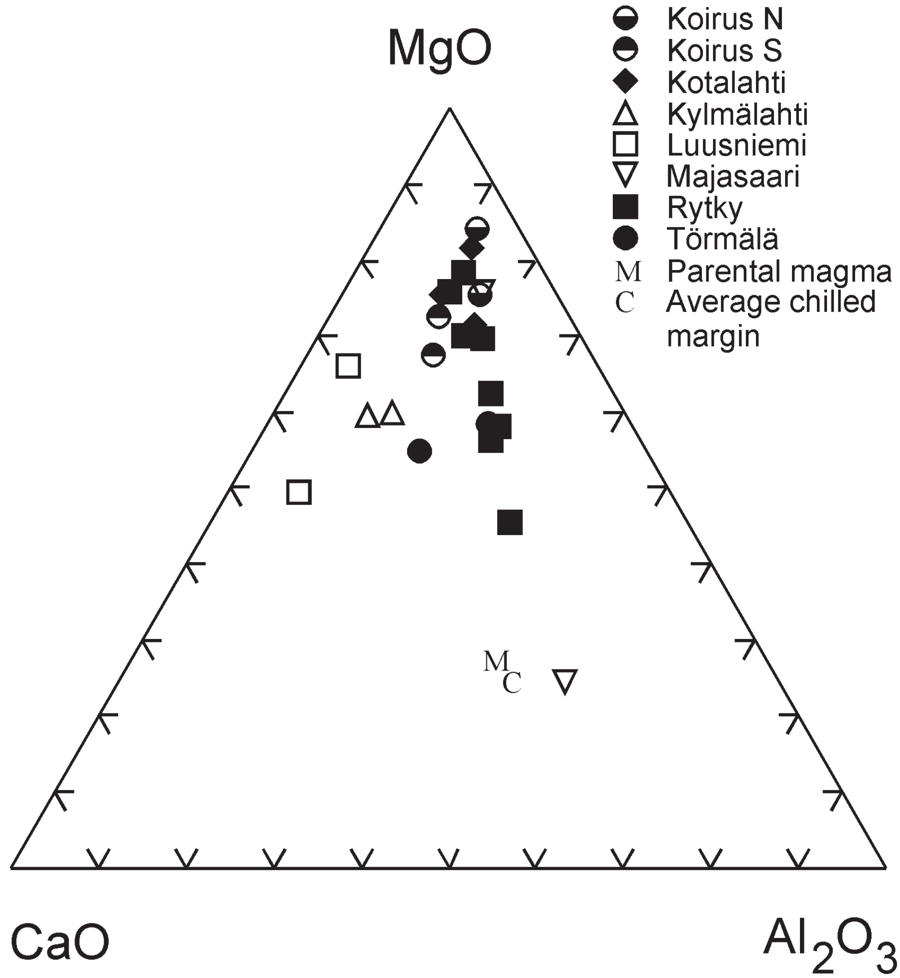

Fig. 2. CMA diagram for the studied samples. Parental magma and chilled margin compositions are from Table 2. Mineralized intrusions indicated by a closed symbol, intermediate intrusions by a half closed symbol and barren intrusions by an open symbol.

areas in the SE part of the Kotalahti Nickel Belt. Ultramafic metavolcanic rocks (metapicrites) occurring together with metabasalts have been described from the same areas (e.g. Gaál & Rauhamäki, 1971; Kousa, 1985; Viluksela, 1988; Makkonen, 1992, 1996). In the Vammala Nickel Belt, only metapicrites (cortlandites) have been described (Häkli et al., 1979; Peltonen, 1990, 1995b). However, Kilpeläinen (1998) proposed that some amphibolites may be cogenetic with the Vammala Belt nickel-bearing intrusions. Lamberg (2005) estimated parental magma compositions for the Laukunkangas intrusion (Kotalahti Belt) and several Vammala Belt intrusions, with the MgO contents ranging between 6.6 and 12.5 wt.%.

Makkonen (1992, 1996) concluded that the metapicrites are metabasalts containing abundant phenocrystic olivine and that the accumulation of olivine took place in flow conduits or during eruption. Nickel mineralization is present in metapicrites at Juva and Rantasalmi and northwest of Mikkeli (Outokumpu Oy, Makkonen, 1984, 1992, 1996; Laitakari, 1985). Geological evidence supporting the genetic relationship between the nickel-bearing intrusions and metapicrites are found in Juva area,

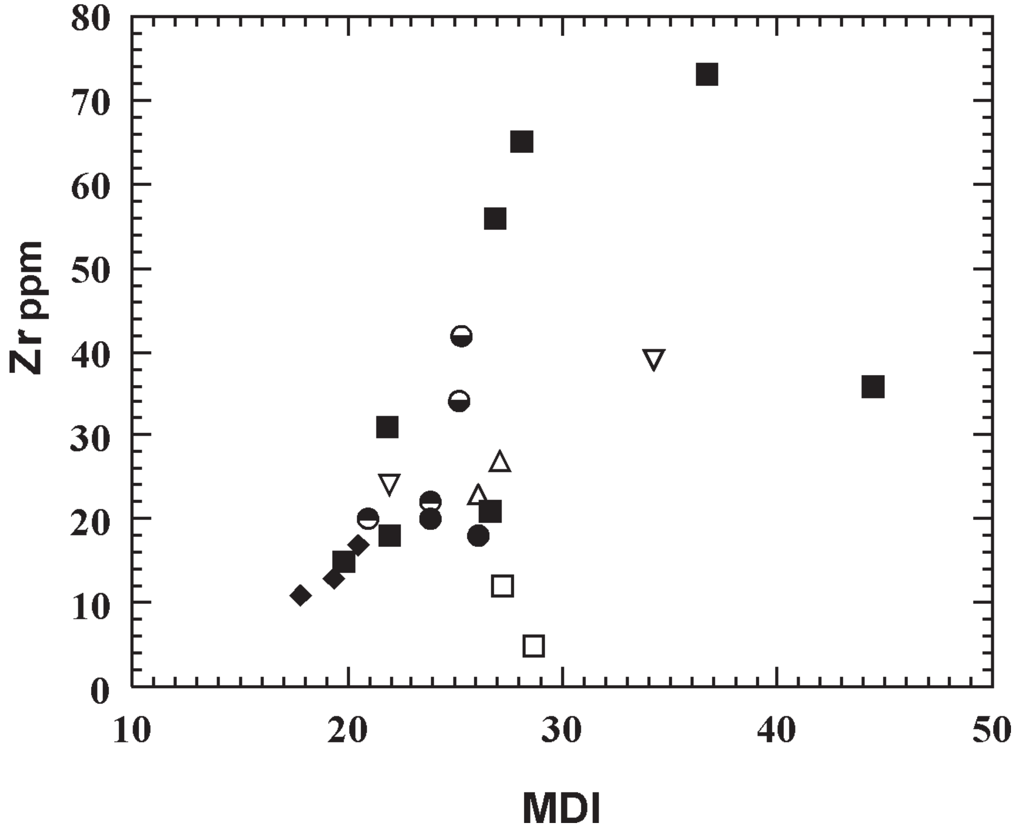

Fig. 3. Zr vs. MDI diagram. Symbols as in Fig. 2. Modified differentiation index (MDI) is calculated from the CIPW normative mineral composition (Gruenewaldt, 1973). MDI = quartz+ orthoclase+albite+diopside*+ferrosilite+fayalite+nepheline+leucite, in which diopside* = 1.88052 x (ferrosilite of diopside).

where within a single linear belt of nickel deposits (Rantala-Honkamäki-Kiiskilänkangas), the host rock of the nickel mineralization ranges in composition from metapicrite to intrusive peridotite (Makkonen, 1992, 1996).

Differences in trace element patterns between the metapicrites and intrusions are, however, evident as the latter usually have higher LILE contents and a wider range of trace element abundances (Peltonen, 1995b; Hill et al., 2005). It has been proposed by Hill et al. (2005) that the metapicrites (and associated metabasalts) and nickel-bearing intrusions have a common mantle source but that their magmas evolved along distinct paths.

Table 2 shows an inferred basaltic composition representing the source magma from which the nickel-bearing intrusions were formed, based on whole rock analytical data for metabasalts from the Rantasalmi, Juva and Enonkoski areas (Hill et al., 2005). For comparison, an average of chilled margin compositions from the Kotalahti Belt intrusions and an EMORB composition are also shown.

The proposed parental magma composition is similar to EMORB, as indicated by the EMORB-normalized spidergram (Fig. 5). Compared to the parental magma, the average chilled margin has elevated LILE concentrations and a distinct Nb-Ta depression. Otherwise the form of the profiles is sim-

Table 2. Proposed parental magma composition for the Svecofennian 1.88 Ga nickel-bearing mafic-ultramafic intrusions compared to EMORB and to an average chilled margin of the intrusions in the Kotalahti Nickel Belt

	Parental magma	EMORB	Chilled margin
n	13		6
SiO_2 (wt.%)	46.51	51.20	49.52
TiO_2	1.11	1.69	1.21
Al_2O_3	14.38	16.00	14.96
FeOT	11.88	8.46	9.44
MnO	0.19	0.16	0.18
MgO	9.37	6.90	8.19
CaO	10.49	11.50	10.10
Na_2O	2.57	2.74	2.51
K_2O	0.23	0.43	1.04
P_2O_5	0.09	0.15	0.18
Total	96.83	99.23	97.32
S (ppm)	286		582
Cr	391	330	207
Ni	246	143	79
Co	54		40
Cu	71		41
Zn	89		84
Ba	81	57	309
Rb	4	5.04	28
Sr	200	155	548
V	268		245
Y	22	22	20
Zr	61	73	86
Hf	2	2.03	2
U	0.22	0.18	0.53
Ta	0.48	0.47	0.45
Th	0.41	0.6	1.45
Nb	5.90	8.3	6.75
La	4.97	6.3	14.46
Ce	12.64	15	33.42
Pr	1.97	2.05	4.67
Nd	9.14	9	20.00
Sm	2.74	2.6	4.19
Eu	1.16	0.91	1.30
Gd	3.39	2.97	4.13
Dy	3.73	3.55	3.70
Tb	0.61	0.53	0.65
Ho	0.83	0.79	0.79
Er	2.25	2.31	2.16
Tm	0.34	0.356	0.31
Yb	2.04	2.37	1.97
Lu	0.33	0.354	0.30

Major elements for EMORB after Kerrich & Wyman (1996), trace elements after Sun & McDonough (1989)
Parental magma and chilled margin values from Hill et al. (2005).

ilar. Negative Nb anomalies (Ta data not available) also are evident in the analyses of intrusive cumulates. The average metasedimentary (WK1; Lahtinen, 2000) and Archaean crustal (AC1; Lahtinen, 2000) compositions conform to the form of the intrusive samples in term of their distinct Nb-(Ta) depressions. In the REE pattern (Fig. 4) the LREE enrichment is very clear in the chilled margin compared to the parental magma.

6. Sm-Nd investigations

In order to characterize the origin and evolution of the magma of the mafic-ultramafic intrusions 23 Sm-Nd isotope analyses were made on samples from eight intrusions. One of the main questions to address has been whether the ore-bearing intrusions are distinct from barren ones in terms of their initial Nd isotope composition. The age of the intrusions is close to 1880 Ma, based on U-Pb zircon dating on gabbros from Kotalahti (1883 ± 6 Ma, Gaál, 1980) and other related intrusions, such as Laukunkangas, some 80 km SE of Kotalahti (1880 ± 3 Ma; Huhma, 1986). The Sm-Nd data are technically good and provide ε_{Nd} values at 1880 Ma from -2.4 to +2.0 (Table 3, Fig. 6). These should represent the initial isotopic composition of the rocks, as post-magmatic REE fractionation is considered to have been negligible.

When evaluating the results, an error in ε_{Nd}(1880 Ma) of ca. ±0.4 units should be taken into account. The samples from Törmälä and Majasaari yield distinctly positive values of around +2, and the two analyses from Luusniemi intrusion have ε_{Nd}(1880 Ma) of -2.4. All other data are distinct from these and provide an average value of -0.7 ± 0.3. Excluding two analyses from the Rytky intrusion, all data from Koirus N, Koirus S, Kotalahti, Rytky and Kylmälahti are within error, in the range -0.7 ± 0.3 (Fig. 6). The two intrusions with positive epsilon are clearly confined to the Svecofennian domain. In the immediate vicinity of the Törmälä body occur 1.92 Ga tonalitic gneisses, which are the oldest known rocks in the Svecofennian domain, and which have yielded initial ε_{Nd} values of ca. +3 (Lahtinen & Huhma, 1997). The

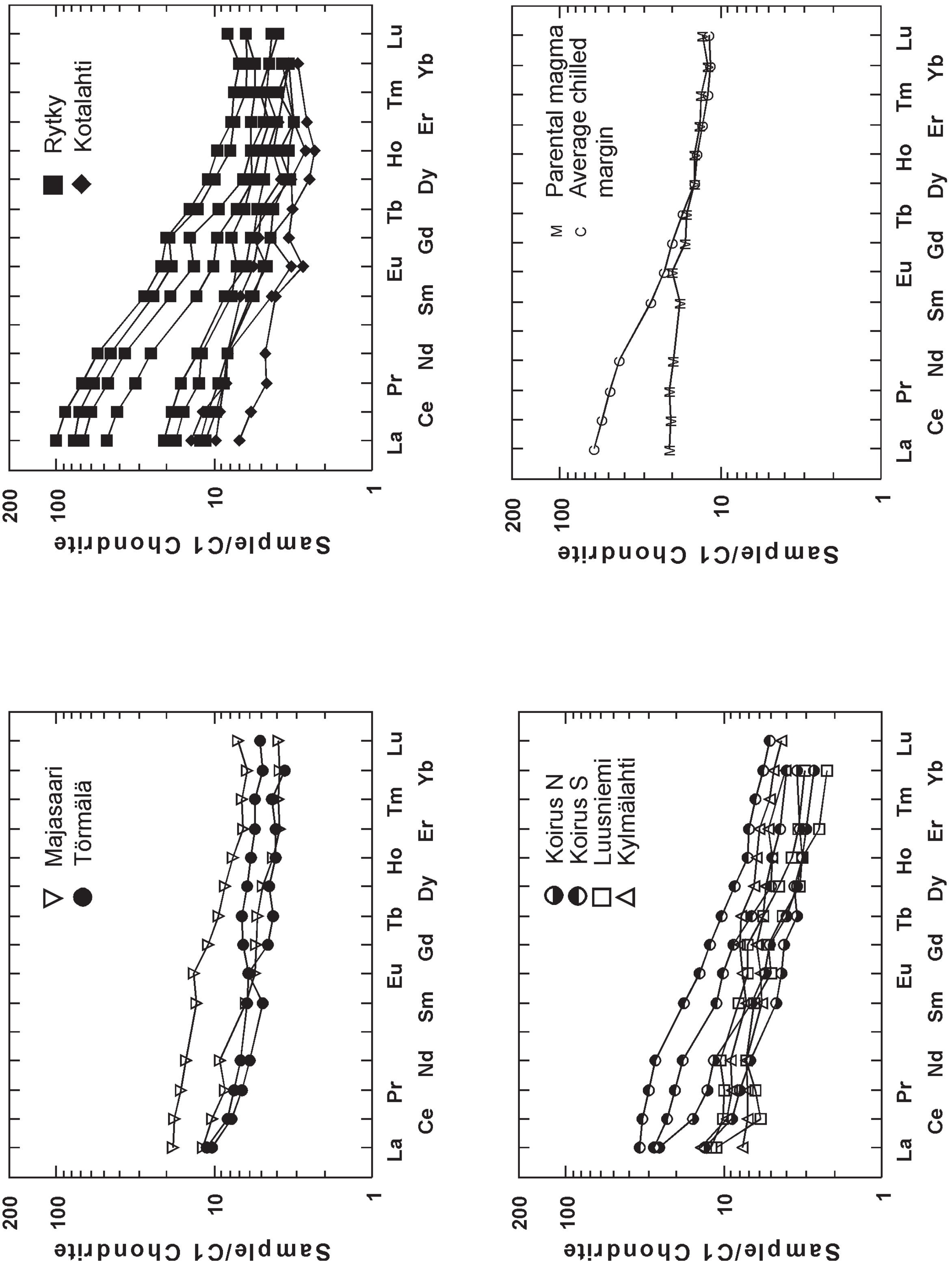

Fig. 4. Chondrite-normalized REE diagrams for intrusions, the proposed parental magma and average chilled margin.

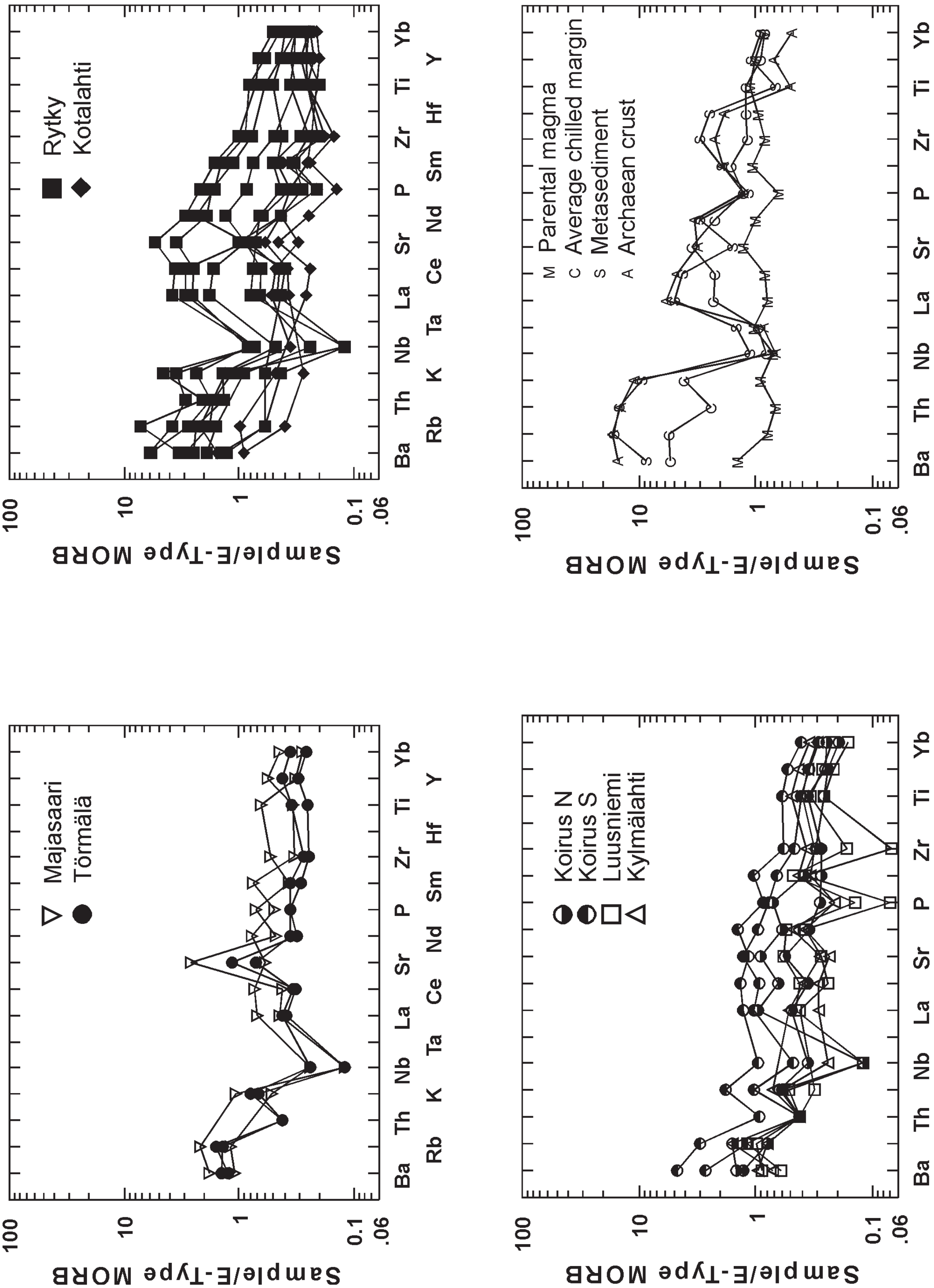

Fig. 5. EMORB-normalized (Sun & McDonough, 1989) spidergrams for intrusions, the proposed parental magma, average chilled margin, average Western Kaleva metasediment (WK1, Lahtinen 2000, table 2) and average Archaean crust (AC1, Lahtinen, 2000, table 2). Because Nb in the study intrusions has been analysed by XRF resulting 1 to 8 ppm, the Nb minimum in the spidergram is only qualitative (comparisons between XRF and ICP-MS Nb analyses have shown that XRF Nb results can however be used below contents of 10 ppm).

Table 3. Sm and Nd concentrations and isotope data. Numbers (1-23) refer to the sample numbers in Table 1.

Number	Sample	Location	Map	Northing	Easting	Ore formation	Rock type	Sm	Nd	$^{147}Sm/^{144}Nd$	$^{143}Nd/^{144}Nd$	2sm	ε(1880 Ma)
								ppm	ppm	(+-0.4%)			(+-0.4)
1	3311R363/97.30	Majasaari	3311	6986186	3445691	barren	Plagioclase-bearing lherzolite	0.98	3.83	0.1550	0.512214	0.000010	1.7
2	3311R363/45.60	Majasaari	3311	6986186	3445691	barren	Olivine gabbronorite	1.93	7.32	0.1594	0.512280	0.000010	2.0
3	3223R312/15.10	Törmälä	3233	6943960	3485961	ore	Olivine gabbronorite	0.82	3.05	0.1619	0.512271	0.000013	1.2
4	3223R312/32.50	Törmälä	3233	6944000	3485886	ore	Olivine gabbronorite	1.02	3.46	0.1776	0.512495	0.000013	1.8
5	KL-468/72.80	Kotalahti	3241	6941498	3531464	ore	Lherzolite. coarse-grained	0.74	3.62	0.1234	0.511675	0.000010	-1.2
6	KL-468/46.30	Kotalahti	3241	6941498	3531464	ore	Lherzolite. medium-grained	0.88	3.44	0.1548	0.512053	0.000010	-1.4
7	KL-817/40.30	Kotalahti	3241	6941673	3531442	ore	Websterite. coarse-grained	0.56	2.23	0.1515	0.512030	0.000010	-1.0
8	3241R460/299.30	Rytky	3241	6940076	3533255	ore	Lherzolite. coarse-grained	2.11	12.15	0.1052	0.511510	0.000010	0.0
9	3241R460/311.45	Rytky	3241	6940076	3533255	ore	Lherzolite. medium-grained	1.23	6.12	0.1215	0.511628	0.000010	-1.6
10	3241R461/116.75	Rytky	3241	6940076	3533255	ore	Melagabbro	4.01	22.44	0.1080	0.511492	0.000010	-1.0
11	3241R473/217.60	Rytky	3241	6940025	3533360	ore	Lherzolite. coarse-grained	3.30	19.67	0.1016	0.511456	0.000010	-0.2
12	3241R473/256.40	Rytky	3241	6940025	3533360	ore	Melagabbro	4.59	26.32	0.1054	0.511472	0.000010	-0.8
13	3241R461/490.00	Rytky	3241	6940076	3533255	ore	Websterite	0.89	3.98	0.1354	0.511834	0.000010	-1.0
14	3241R462/268.80	Rytky	3241	6940128	3533178	ore	Websterite	1.43	5.95	0.1453	0.511969	0.000010	-0.7
15	3241R410/268.50	Rytky	3241	6940191	3532732	ore	Gabbronorite	0.97	3.88	0.1517	0.512103	0.000010	0.4
16	3241R451/299.10	Koirus N	3241	6945700	3535420	intermediate	Olivine-websterite	0.80	3.39	0.1420	0.511967	0.000013	0.0
17	3241R395/36.70	Koirus N	3241	6945900	3536025	intermediate	Serpentinite	1.15	5.64	0.1236	0.511701	0.000011	-0.7
18	3241R398/24.00	Koirus S	3241	6942827	3536114	intermediate	Lherzolite	3.09	14.30	0.1307	0.511793	0.000011	-0.6
19	3241R398/63.20	Koirus S	3241	6942827	3536114	intermediate	Lherzolite	2.00	9.44	0.1282	0.511741	0.000011	-1.0
20	3242R321/272.10	Luusniemi	3242	6951025	3538965	barren	Lherzolite	1.24	4.62	0.1625	0.512096	0.000011	-2.4
21	3242R321/278.30	Luusniemi	3242	6951025	3538965	barren	Lherzolite	0.97	3.19	0.1830	0.512347	0.000011	-2.4
22	3241R306/30.65	Kylmälahti	3241	6933040	3536080	barren	Metaperidotite	1.09	3.60	0.1836	0.512467	0.000013	-0.2
23	3241R307/42.00	Kylmälahti	3241	6933040	3536100	barren	Metaperidotite	1.33	4.54	0.1773	0.512402	0.000028	0.0

Luusniemi intrusion with ε_{Nd}(1880) of -2.4 is located close to the exposed main Archaean basement.

Another objective of the study is to compare the Sm-Nd isotope compositions of ore-bearing and barren intrusions. The ore-bearing intrusions yield average ε_{Nd}(1880 Ma) -values of +1.5 ± 0.4 (Törmälä), -1.2 ± 0.2 (Kotalahti) and -0.6 ± 0.5 (Rytky), the intermediate Koirus bodies give an average value of -0.6 ± 0.5, and the barren intrusions have ε_{Nd}(1880 Ma) of -2.4 ± 0.2 (Luusniemi), -0.1 ± 0.4 (Kylmälahti) and +1.9 ± 0.3 (Majasaari). Consequently, no relationship has been found between the degree of nickel mineralization and initial ε_{Nd} values.

7. Discussion

Previous Sm-Nd studies have shown that depleted mantle with ε_{Nd} values close to + 4 at approximately 2.0 Ga was the source for several mafic-ultramafic rocks in the Fennoscandian Shield (e.g. Huhma et al., 1990; Hanski et al., 2001b; Hanski & Huhma, 2005). Further evidence for a major contribution from such sources is provided by the 1.92 Ga juvenile felsic crust in the Kotalahti Nickel Belt, which is characterized by initial epsilon values of ca. + 3 (Lahtinen & Huhma, 1997). If the parental magma for the Svecofennian nickel-bearing intrusions was similar to the proposed magma in Table 2, then the intrusions could also have been derived from a depleted mantle source with initial epsilon values near + 4.

The Sm-Nd data for the Svecofennian metapicrites/metabasalts and mafic-ultramafic intrusions are shown in Fig. 8, and include several previously unpublished analyses (see also Appendix 1). The data for the intrusions seem to plot into two groups. A number of intrusions yield ε_{Nd}(1880Ma) -values close to 0 (Laukunkangas, Juva, Stormi, Porrasniemi), whereas others yield distinctly positive values up to +3 (Ylivieska, Hyvinkää, Juva, Parikkala).

It is evident that many mafic-ultramafic rocks provide much lower initial epsilon values than the depleted mantle value discussed above, which implies the existence of mantle heterogeneity or the involvement of crustal contamination in their genesis. Alkaline rocks with high REE abundances and ε_{Nd} values close to zero evidently suggest that mantle contained isolated reservoirs with distinct isotopic compositions (e.g. Peltonen et al., 1996). High degrees of enrichment can occur within mantle plumes, and metasomatized continental lithospheric mantle sources can generate low initial values. On the other hand, several lines of evidence show that assimilation of crustal material has had a major influence on the evolution of mantle-derived magmas. However, the nature and timing of the contamination processes have in many instances remained obscure. In the present study area, interpretations have been presented that range from *in situ* contamination (Mäkinen & Makkonen, 2004; Makkonen et al., 2007) to source contamination, *i.e.* assimilation of crustal material at great depth in a subduction zone environment (Patchett & Kouvo, 1986).

In the present case, geological evidence is available to assist in evaluating the relative importance of mantle heterogeneity or crustal contamination. The most important finding is that the intrusions having the lowest ε_{Nd} values occur close to the Archaean granitoids (ε_{Nd} ca. -10), while the intrusions having the highest ε_{Nd} values occur within granitoids having ε_{Nd} ca. +3. Thus the ε_{Nd} values of the intrusions correlate with the ε_{Nd} values of the country rocks, which suggests that crustal contamination was a more likely process. Many earlier studies of Svecofennian 1.88 Ga mafic-ultramafic have also presented evidence for crustal contamination (e.g. Peltonen, 1995a, 1995b, 2005; Mäkinen & Makkonen, 2004; Makkonen, 1996; Lamberg, 2005; Makkonen et al., 2007). Mäkinen & Makkonen (2004) found that in the Rytky intrusion, the first and the most primitive intrusive phase (represented by the coarse-grained lherzolite) was the most contaminated. In Fig. 7, ε_{Nd} is plotted against MgO and Al_2O_3 for the Rytky and Kotalahti samples. These two intrusions have similar rock types and wall rocks (Mäkinen & Makkonen, 2004). The lowest ε_{Nd} values tend to be in the samples richest in MgO and poorest in Al_2O_3, which is in agreement with the conclusion of Mäkinen & Makkonen (2004). The high degree of contamination in the MgO-rich rocks can be explained by the high la-

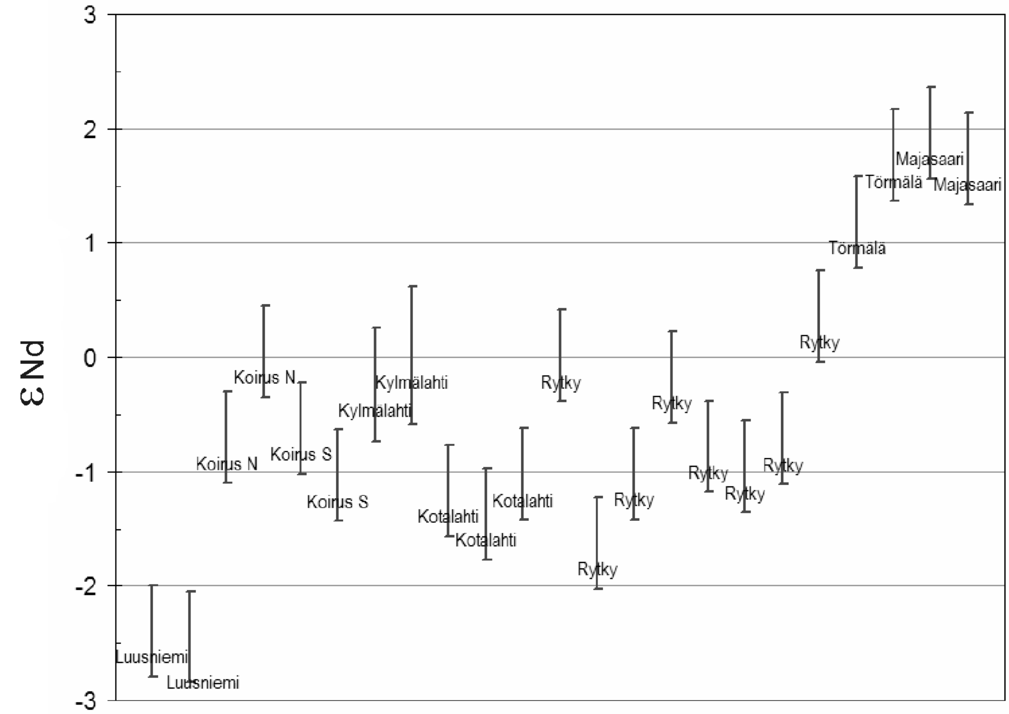

Fig .6. ε_{Nd} values for each sample calculated at 1880 Ma. The Luusniemi intrusion is located closest to the exposed main Archaean domain, while the Törmälä and Majasaari intrusions are located furthest away. Other intrusions lie within the transition zone between the Archaean and Proterozoic rocks. Error bars are 2-sigma.

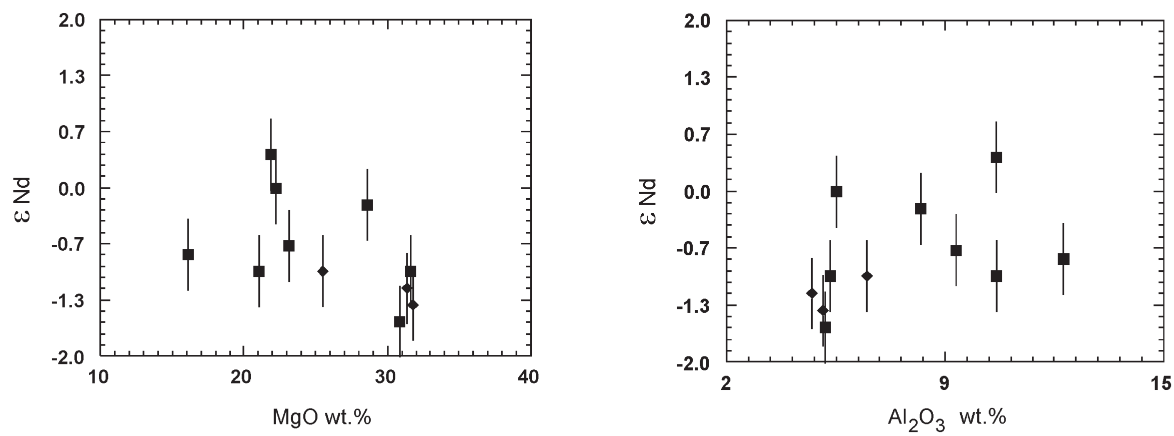

Fig. 7. ε_{Nd}(1880 Ma) vs. MgO (vol. free) and ε_{Nd}(1880 Ma) vs. Al_2O_3 (vol. free) diagrams for Rytky (square) and Kotalahti (diamond) samples. Error bars (+/- 0.4) marked.

tent heat of the crystallization of MgO-rich cumulates and therefore an increased ability to assimilate wall rock material. This interpretation is also consistent with a crustal origin for the low ε_{Nd} values. Mantle-derived values should not be expected to display any correlation with magmatic differentiation.

The trace element contents of the intrusions and the proposed parental magma will now be considered in further detail. The differences between the intrusion sample compositions and the inferred parental magma, notably, the Nb-(Ta) depression in the spider diagrams and the negative slopes for LREE of the intrusive samples are both typical of crustally contaminated rocks (cf. Figs. 4 and 5). On the other hand, negative Nb anomalies are also characteristic features of subduction-related magmas. This kind of anomaly is generally attributed to decoupling of Nb from incompatible elements such as Th and Ce during dehydration and partial melting of subducted oceanic lithosphere. Thorium and Ce are transferred by fluids derived from the subducting plate to the sub-arc mantle wedge, whereas Nb is preferentially retained in the subducting slab by amphibole + titanite and rutile (Pearce, 1996). Thus, there are two alternative mechanisms for generating the negative Nb anomalies: 1) selective contamination in the subduction zone (source contamination) and 2) contamination in the crust.

The abundance of Zr and Zr/Ti ratios have been used to indicate the presence of crustal contamination in Svecofennian mafic-ultramafic intrusions (Makkonen, 1996; Makkonen & Mäkinen, 2003; Mäkinen & Makkonen, 2004; Makkonen et al., 2007). Because Zr is an incompatible element it should have a much lower concentration in an ultramafic cumulate than in the respective magma. However in many of the studied intrusions, especially in Rytky, the Zr content in ultramafic cumulates can attain typical magmatic values (cf. Tables 1 and 2 and Fig. 3). The most typical country rock for the intrusions, mica gneiss, contains three to four times more Zr than the parental magma (an average of 217 ppm from 47 samples after Lahtinen (2000) and an average of 184 ppm from 72 samples after Makkonen et al. (2007). Assimilation of mica gneiss thus effectively increases the Zr content of the magma. Archaean crust has an average Zr content of 162 ppm (129 samples, Lahtinen, 2000), being thus comparable to the Proterozoic mica gneisses. The 1.93 – 1.91 Ga gneissic tonalites surrounding the Törmälä intrusion also have similar Zr values (Lahtinen, 1994).

Although mantle heterogeneity as an explanation for the range of the initial ε_{Nd}-values cannot be entirely excluded, on the basis of the above discussion, we conclude that interaction with crustal rocks is the most probable explanation for the low initial ε_{Nd} values of the studied intrusions. Because there is a general geochemical correlation with the geological environment (juvenile crust vs. Archaean domain) and with the country rock (not necessarily intrusion wall rock), contamination probably took place in the upper crust. The elevated contents of Rb and Th, which have higher abundances in the upper than in the lower crust (Wilson, 1993), also favour the upper crust as the principal contaminant. In Fig. 8 Sm-Nd isotope data for Svecofennian mafic-ultramafic intrusions are compared with those of the metapicrites/metabasalts representing the proposed parental magma and also with Svecofennian metasediments and Archaean rocks in Finland. The studied intrusions of the Kotalahti area plot away from the parental magma composition towards the metasediments and Archaean rocks, while the Majasaari and Törmälä intrusions correspond more closely to the magmatic composition. The intrusions in the Kotalahti area have low initial ε_{Nd} values compared to other Svecofennian intrusions and the inferred parental magma composition (metapicrites/metabasalts), consistent with the proposed contamination by Archaean granitoids and Svecofennian metasediments.

A simple crustal contamination model involves bulk mixing of a magma and contaminant. However, in many cases this approach has proven unsatisfactory, in that different elements giving mutually conflicting results with respect to the degree of contamination. More sophisticated models take into account the effects of combined assimilation of crust, fractional crystallisation, magma recharge and eruption

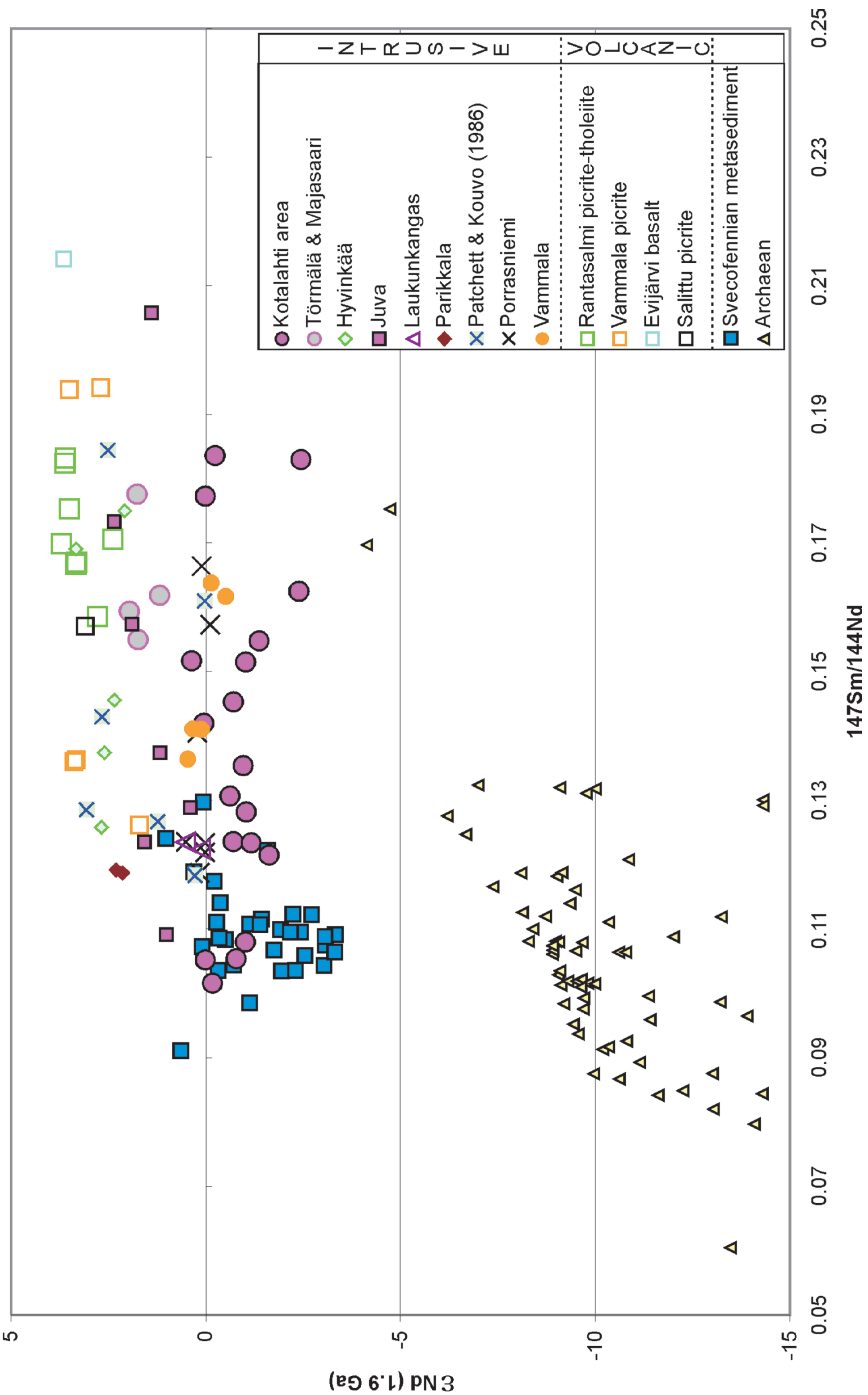

Fig. 8. Sm-Nd isotope data for Svecofennian mafic-ultramafic intrusions, metapicrites and metabasalts representing the proposed parental magma and Svecofennian metasediments as well as Archaean felsic rocks in Finland. Data from Huhma (1986, 1987), Patchett & Kouvo (1986), Makkonen (1996), Lahtinen et al. (2002), Lamberg (2005), Jahn et al. (1984), Hanski et al. (2001a), O'Brien et al. (1993), Hölttä et al. (2000), Mutanen & Huhma (2003), Lauri et al. (2006), Halla (2002), Käpyaho et al. (2006).

(Aitcheson & Forrest, 1994). In the AFC process (Assimilation and Fractional Crystallisation, DePaolo, 1981), contamination is accompanied by concurrent fractional crystallization and this is widely considered to occur in magma chambers, where the heat released by crystallization allows fusion of wall rocks (Wilson, 1993). In the AFC process, the most fractionated rocks should be most contaminated, because the residual melt has a longer time to interact with the contaminant than the melt represented by the early cumulates. In contrast, Devey & Cox (1987) described an AEC process (Assimilation and Equilibrium Crystallisation), in which crystallisation and assimilation proceed together but fractionation is suppressed. Such a process is envisaged to occur during magma ascent rather than within a magma chamber and produces a positive correlation between the degree of contamination and the Mg-number, because of the higher temperature of the most primitive intrusion phase.

The results of this study are more consistent with an AEC process than an AFC process since the most MgO-rich cumulates in Rytky and Kotalahti tend to have the lowest ε_{Nd} values (cf. Fig. 7). A similar type of contamination is also found in some other Svecofennian intrusions, where the Zr content in peridotite is higher than in gabbro (Makkonen, 1996). If the AEC process is accepted, then *in situ* contamination should probably be neglected, because the AEC process rather takes place in a magma conduit. On the other hand, in the Rytky intrusion, according to Mäkinen & Makkonen (2004), the magma chamber was still open during the first magma pulse. Therefore, magma could have been actively flowing through the chamber with conditions probably more like in a flow conduit than in the final closed chamber. In the case of the Luusniemi intrusion however, contamination during magma ascent is suggested. This intrusion has the lowest ε_{Nd} value, although the *wall rock* is not Archaean gneiss. Consequently, the magma forming the Luusniemi intrusion has passed through Archaean rocks below the present erosion level. This is in accord with the observation that Archaean gneiss some 2 km NW of the Luusniemi intrusion plunges to SE under the intrusion (Mäkinen, pers.comm., 2006).

If an AFC process was not important in the contamination event, bulk contamination calculations (Table 4) can be used to evaluate the amount of assimilated crust. The bulk distribution coefficient of Nd for ultramafic cumulates is very low (≤ 0.1), which makes the difference between the AFC and bulk contamination calculations small (Aitcheson & Forrest, 1994). As can be seen from Table 4, to obtain a negative ε_{Nd} (1880 Ma) value for the studied intrusions, bulk contamination of about 10 % by Archaean gneiss and about 30 % by Svecofennian metasediment is required (similar results were obtained also by Patchett & Kouvo, 1986 and Huhma, 1986). In the case where only 10 % contamination has taken place the overall changes in trace element compositions are small. This, together with a small amount of intercumulus liquid, may explain the low incompatible element concentrations of the Luusniemi intrusion compared to other intrusions. In other words, the low trace element content coupled with the most negative ε_{Nd} (1880 Ma) value in the Luusniemi intrusion suggests a contamination process involving mainly Archaean gneiss material.

For comparison, in a recent study of the Ni-Cu-PGE bearing Expo Intrusive Suite (1.88 Ga) in the Cape Smith Fold Belt, New Quebec, Mungall (2007) concluded that the amount of assimilated upper crust in many cases was about 15 % with a maximum of up to 50 % by mass. Makkonen (1996) estimated the amount of crustal assimilation to be 5 – 40 % by mass in the Juva area in the Kotalahti Nickel Belt (1.88 Ga).

Considering the calculated results of a simple bulk contamination process, one must bear in mind that some variation in the contamination processes between the intrusions is probable. It is likely that the processes were complex, since several phases of contamination could have occurred during passage of the magma through the feeder channels before reaching its final site of emplacement. Contamination could also have been somewhat selective. Thus, some of the differences in the observed whole-rock geochemical

Table 4. Variations in εNd (1880 Ma) values in a bulk mixing process.

Mixture of Archaean gneiss with εNd -10 and magma with εNd +3.7			Mixture of Svecofennian gneiss with εNd - 2 or -3.3 and magma with εNd +3.7			
Proportion of Archaean gneiss	Proportion of magma	εNd Mixture	Proportion of Svecof. gneiss	Proportion of magma	εNd Mixture	
Nd 30 ppm	Nd 9.14 ppm		Nd 30 ppm	Nd 9.14 ppm	εNd -2	εNd -3.3
0.01	0.99	3.3	0.01	0.99	3.5	3.5
0.02	0.98	2.8	0.02	0.98	3.3	3.3
0.03	0.97	2.4	0.03	0.97	3.2	3.1
0.04	0.96	2.1	0.04	0.96	3.0	2.9
0.05	0.95	1.7	0.05	0.95	2.9	2.7
0.06	0.94	1.3	0.06	0.94	2.7	2.5
0.07	0.93	1.0	0.07	0.93	2.6	2.3
0.08	0.92	0.7	0.08	0.92	2.4	2.1
0.09	0.91	0.3	0.09	0.91	2.3	2.0
0.10	0.90	0.0	0.10	0.90	2.2	1.8
0.15	0.85	-1.3	0.15	0.85	1.6	1.1
0.20	0.80	-2.5	0.20	0.80	1.1	0.5
0.25	0.75	-3.5	0.25	0.75	0.7	0.0
0.30	0.70	-4.3	0.30	0.70	0.4	-0.4

features indicating contamination may reflect differences in the contamination process.

One of the purposes of this study was to compare the Sm-Nd isotope compositions of the mineralized and barren intrusions, *i.e.* to investigate whether the mineralized intrusions have lower ε_{Nd} (1880 Ma) values than the barren ones. This might be the case if contamination of (sulfide-bearing) sediments was a major cause for mineralization. However, no such relationship could be found. This is partly because there were two main types of contaminants: Archaean gneiss with an ε_{Nd} (1880 Ma) value of about -10 and Svecofennian metasediment with an ε_{Nd} (1880 Ma) value of about -2. Thus the differences in the ε_{Nd} (1880 Ma) values result mainly from the contaminant type and not from the amount of contamination.

7. 1. Tectonic implications

The results of this study provide additional information on the Archaean/Proterozoic boundary in the Kotalahti Nickel Belt. Many authors have modelled the evolution of the Archaean/Proterozoic boundary and presented different views on the direction of the possible subduction (e.g. Gaál, 1982, 1986, 1990; Ward, 1987; Ekdahl, 1993; Lahtinen, 1994; Ruotoistenmäki, 1996; Nironen, 1997; Lahtinen et al., 2005). On the basis of the fact that Archaean influence (low ε_{Nd} value) is controlled by the Archaean/Proterozoic contact at the *present* erosion level and assuming that the magma conduit in the upper crust was vertical to subvertical, we can assume that the Archaean basement was not present further west at deeper levels during magma ascent at 1880 Ma.

The metatholeiites representing the parental magma for the Svecofennian nickel-bearing intrusions occur in the Savo area together with limestones, cherts and iron formations and commonly exhibit pillow structures. These features, together with the fact that the tholeiitic magmas have an EMORB affinity, suggests a cratonic margin or marginal basin environment for eruption - e.g. a back arc setting. Similarly, Viluksela (1988) proposed a back arc basin environment for the Rantasalmi tholeiites and picrites. Metapicrites genetically related to the metatholeiites are abundant all around the Central Finland Granitoid Complex (CFGC). This is in accord with the presence of nickel-bearing intrusions around the CFGC, an observation already noted in the 1970's (Häkli, 1971; Häkli et al., 1979). Consequently, it is reasonable to propose an episode of rifting near the craton margin, accompanied by widespread mafic volcanism. Slightly later (at 1.88 Ga), during the main Svecofennian collisional and tectonic thickening stage (cf. Makkonen, 2005), the mafic magma formed nickel-bearing intrusions within the Svecofennian sediments, craton margin sequence and Archaean gneisses.

The results of this study provide some useful insights with respect to nickel exploration: 1) The Sm-Nd isotope data are compatible with the view that the metatholeiite-metapicrite series represents the parental magma for the nickel-bearing intrusions and therefore, the geochemistry of the metatholeiites/metapicrites can be used in nickel exploration. 2) Because the wall rock Sm-Nd isotopic composition does not necessarily correlate with that of the intrusion, crustal contamination has also taken place during magma ascent, either in flow conduits or in intermediate magma chambers. Therefore, in such cases sulfide segregation has probably taken place before the final emplacement of the magma, as also proposed by Peltonen (1995a, 1995b, 2005) and Lamberg (2005).

8. Conclusions

1) The Sm-Nd data for the eight intrusions provide initial ε_{Nd} values at 1880 Ma from -2.4 to +2.0.

2) Initial ε_{Nd} values of the intrusions correlate with the geological domain and the country rock type. The Majasaari and Törmälä intrusions, with positive ε_{Nd} values, occur within the Svecofennian domain, in proximity to juvenile 1.92 Ga tonalitic gneisses, which have yielded initial ε_{Nd} values of ca. +3. The Luusniemi intrusion with ε_{Nd} -2.4 is located close to exposed Archaean crust. Although mantle heterogeneity as an alternative explanation for the range of the initial ε_{Nd} values cannot be entirely excluded, the results support the concept of contamination by Archaean material in proximity to the currently exposed craton margin, while militating against the presence of buried Archaean crust further west at 1.88 Ga. No relationship can be found between nickel mineralization and initial ε_{Nd} values. This is partly because the differences in the ε_{Nd} (1880 Ma) values result mainly from the contaminant type (Archaen gneiss/Svecofennian metasediment) and not from the amount of contamination.

3) The average composition of the metabasalts in the southern Savo area is considered to be equivalent to the parental magma for the intrusions, composition of this magma being close to EMORB. Metapicrites occurring widely around the Central Finland Granitoid are cogenetic with the metabasalts. The initial ε_{Nd} values for the metapicrites are near +4 suggesting a depleted mantle source for the parental magma. The higher MgO content of the metapicrites is due to olivine accumulation.

4) A simple bulk-mixing model between the parental magma and Svecofennian metasediment/Archaean gneiss yields initial ε_{Nd} values similar to those obtained from the intrusion samples. Assimilation of about 20 % of Archaean gneiss is required to produce the lowest obtained initial ε_{Nd} value (-2.4).

Acknowledgements

We thank Eero Hanski and an anonymous reviewer for the constructive suggestions, which greatly improved this paper and Peter Sorjonen-Ward for language checking.

References

Aitcheson, S.J. & Forrest, A.H., 1994. Quantification of crustal contamination in open magmatic systems. Journal of Petrology 35, 461–488.

DePaolo, D.J., 1981. Neodymium isotopes in the Colorado Front Range and crust-mantle evolution in the Proterozoic. Nature 291, 684–687.

Devey, C.W. & Cox, K.G., 1987. Relationships between crustal contamination and crystallization in continental flood basalt magmas with special reference to the Deccan Traps of the Western Ghatts, India. Earth and Planetary Science Letters 84, 59–68.

Ekdahl, E., 1993. Early Proterozoic Karelian and Svecofennian formations and the evolution of the Raahe-Ladoga Ore Zone, based on the Pielavesi area, central Finland. Geological Survey of Finland, Bulletin 373, 137 p.

Forss, H., Kontoniemi, O., Lempiäinen, R., Luukas, J., Makkonen, H. & Mäkinen, J., 1999. Ni-vyöhyke ja 1. 9 Ga magmatismi-hankkeen (12204) toiminta vuosina 1992-1998 Tervo-Varkaus-alueella. Geological Survey of Finland, Archive report, M 19/3241/99/1/10, 152 p.

Gaál, G., 1972. Tectonic control of some Ni-Cu deposits in Finland. In: Gill, J. E. (ed.) International Geological Congress, 24th session, Montreal 1972: Section 4, Mineral deposits, pp. 215–224.

Gaál, G., 1980. Geological setting and intrusion tectonics of the Kotalahti nickel-copper deposit, Finland. Bulletin of the Geological Society of Finland 52, 101–128.

Gaál, G., 1982. Proterozoic tectonic evolution and late Svecokarelian plate deformation of the central Baltic Shield. Geologische Rundschau 71, 158–170.

Gaál, G.1986. 2200 million years of crustal evolution: the Baltic Shield. Bulletin of the Geological Society of Finland 58, 149–168.

Gaál, G. 1990. Tectonic styles of Early Proterozoic ore deposition in the Fennoscandian Shield. Precambrian Research 46, 83–114.

Gaál, G. & Rauhamäki, E., 1971. Petrological and structural analysis of the Haukivesi area between Varkaus and Savonlinna, Finland. Bulletin of the Geological Society of Finland 43, 265–337.

Gruenewaldt, G. Von, 1973. The modified differentiation index and the modified crystallization index as parameters of differentiation in layered intrusions. Transactions of the Geological Society of South Africa 76, 53–61.

Häkli, T.A., 1971. Silicate nickel and its application to the exploration of nickel ores. Bulletin of the Geological Society of Finland 43, 247–263.

Häkli, T.A., Vormisto, K. & Hänninen, E., 1979. Vammala, a nickel deposit in layered ultramafite, Southwest Finland. Economic Geology 74, 1166–1182.

Halla, J., 2002. Origin and Paleoproterozoic reactivation of NeoArchaean high-K granitoid rocks in eastern Finland. Annales Academiae Scientiarum Fennicae, Geologica-Geographica 163. Academica Scientiarum Fennica, Helsinki, 103 p.

Hanski, E., Walker, R.J., Huhma, H. & Suominen, I., 2001a. The Os and Nd isotopic systematics of the c. 2.44 Ga Akanvaara and Koitelainen mafic layered intrusions in northern Finland. Precambrian Research. 109, 73–102.

Hanski, E., Huhma, H. & Vaasjoki, M., 2001b. Geochronology of northern Finland: a summary and discussion. In: Vaasjoki, M. (ed.) Radiometric age determinations from Finnish Lapland and their bearing on the timing of Precambrian volcano-sedimentary sequences. Geological Survey of Finland, Special Paper 33, 255–279.

Hanski, E. & Huhma, H., 2005. Central Lapland greenstone belt. In: Lehtinen, M., Nurmi, P. A. & Rämö, O. T. (eds.) Precambrian geology of Finland – Key to the evolution of the Fennoscandian Shield. Developments in Precambrian Geology 14, Elsevier, Amsterdam, pp. 139–193.

Haughton, D.R., Roeder, P.L. & Skinner, B.J., 1974. Solubility of sulfur in mafic magmas. Economic Geology 69, 451–467.

Hill, R., Barnes, S., Dowling, S., Makkonen, H. & Peltonen, P., 2005. Chalcophile element distribution in mafic and ultramafic metavolcanic rocks of the Svecofennian Kotalahti and Vammala Nickel Belts Finland – A test for a geochemical signature of subvolcanic magmatic ore forming processes. Regional area selection criteria for intrusive Ni/Cu sulfide ore deposits. Final report, CSIRO, GTK. Geological Survey of Finland, Archive report, M 10.4/2005/2, 217 p.

Hölttä, P., Huhma, H., Mänttäri, I. & Paavola, J., 2000. P-T-t development of Archaean granulites in Varpaisjärvi, Central Finland, II: Dating of high-grade metamorphism with the U-Pb and Sm-Nd methods. Lithos 50, 121–136.

Huhma, H., 1986. Sm-Nd, U-Pb and Pb-Pb isotopic evidence for the origin of the Early Proterozoic Svecokarelian crust in Finland. Geological Survey of Finland, Bulletin 337, 48 p.

Huhma, H., Cliff, R.A., Perttunen, V. & Sakko, M., 1990. Sm-Nd and Pb isotopic study of mafic rocks associated with early Proterozoic continental rifting: the Peräpohja schist belt in northern Finland. Contributions to Mineralogy and Petrology 104, 367–379.

Jahn, B-M., Vidal, P. and Kröner, A., 1984. Multi-chronometric ages and origin of Archaean tonalitic gneisses in Finnish Lapland: a case for long crustal residence time. Contributions to Mineralogy and Petrology 86, 398–408.

Käpyaho, A., Mänttäri, I. & Huhma, H., 2006. Growth of Archaean crust in the Kuhmo district, eastern Finland: U–Pb and Sm–Nd isotope constraints on plutonic rocks. Precambrian Research 146, 95–119.

Kerrich, R. & Wyman, D.A., 1996. The trace element systematics of igneous rocks in mineral exploration: an overview. In Wyman, W.A. (ed.) Trace element geochemistry of volcanic rocks: applications for massive sulphide exploration. Geological Association of Canada, Short Course Notes 12, 1–50.

Kilpeläinen, T., 1998. Evolution and 3D modelling of structural and metamorphic patterns of the Palaeoproterozoic crust in the Tampere-Vammala area, southern Finland. Geological Survey of Finland, Bulletin 397, 124 p.

Koistinen, T.J., 1981. Structural evolution of an early Proterozoic stratabound Cu-Co-Zn deposit, Outokumpu, Finland. Transactions of the Royal Society of Edinburgh: Earth Sciences 72, 115–158.

Korsman, K., Koistinen, T., Kohonen, J., Wennerström, M., Ekdahl, E., Honkamo, M., Idman, H. & Pekkala, Y. (eds.), 1997. Suomen kallioperäkartta/Bedrock map of Finland 1:1 000 000. Geological Survey of Finland, Espoo.

Kousa, J., 1985. Rantasalmen tholeiittisista ja komatiittisista vulkaniiteista. Summary: The tholeiitic and komatiitic metavolcanics in Rantasalmi, Southeastern Finland. Geologi 37, 17–22.

Kousa, J. & Lundqvist, Th., 2000. Meso- and Neoproterozoic cover rocks of the Svecofennian Domain. In: Lundqvist, Th. & Autio, S. (eds.) Description to the bedrock map of central Fennoscandia (Mid-Norden). Geological Survey of Finland, Special Paper 28, 75–76.

Lahtinen, R., 1994. Crustal evolution of the Svecofennian and Karelian domains during 2.1-1.79 Ga, with special emphasis on the geochemistry and origin of 1.93-1.91 Ga gneissic tonalites and associated supracrustal rocks in the Rautalampi area, central Finland. Geological Survey of Finland, Bulletin 378, 128 p.

Lahtinen, R., 2000. Archaean-Proterozoic transition: geochemistry, provenance and tectonic setting of metasedimentary rocks in central Fennoscandian Shield, Finland. Precambrian Research 104, 147–174.

Lahtinen, R. & Huhma, H., 1997. Isotopic and geochemical constraints on the evolution of the 1.93-1.79 Ga Svecofennian crust and mantle in Finland. Precambrian Research 82, 13–34.

Lahtinen, R., Huhma, H. & Kousa, J., 2002. Contrasting source components of the Paleoproterozoic Svecofennian metasediments: detrital zircon U-Pb, Sm-Nd and geochemical data. Precambrian Research 116, 81–109.

Lahtinen, R., Korja, A. & Nironen, M., 2005. Paleoproterozoic tectonic evolution. In: Lehtinen, M., Nurmi, P. A. & Rämö, O. T. (eds.) Precambrian geology of Finland – Key to the evolution of the Fennoscandian Shield. Developments in Precambrian Geology 14, Elsevier, Amsterdam, pp. 481–531.

Laitakari, A.J., 1985. Tutkimustyöselostus Mikkelin mlk:ssa valtausalueilla Korpijärvi 1, kaiv.rek.n:o 2978/1 sekä Iso-Mietiäinen 1, kaiv.rek.n:o 2978/2 ja Iso-Mietiäinen 2, kaiv.rek.n:o 2978/3 suoritetuista tutk. Geological Survey of Finland, Archive report, M06/3142/-85/1, 8 p.

Lamberg, P., 2005. From genetic concepts to practice – lithogeochemical identification of Ni-Cu mineralised intrusions and localisation of the ore. Geological Survey of Finland, Bulletin 402, 264 p.

Lauri, L.S., Rämö, O.T., Huhma, H., Mänttäri, I. & Räsänen, J., 2006. Petrogenesis of silicic magmatism related to the ~2.44 rifting of Archaean crust in Koillismaa, eastern Finland. Lithos 86, 137–166.

Ludwig, K.R., 2001. Users Manual for Isoplot/Ex rev. 2.49. Berkeley Geochronological Center, Special Publication No. 1a, 55 p.

Mäkinen, J., 1987. Geochemical characteristics of Svecokarelidic mafic-ultramafic intrusions associated with Ni-Cu occurrences in Finland. Geological Survey of Finland, Bulletin 342, 109 p.

Mäkinen, J. & Makkonen, H.V., 2004. Petrology and structure of the Palaeoproterozoic (1.9 Ga) Rytky nickel sulphide deposit, Central Finland: a comparison with the Kotalahti nickel deposit. Mineralium Deposita 39, 405–421.

Makkonen, H. 1984. Tutkimustyöselostus Juvan kunnassa valtausalueella Rantala 1, kaiv. rek. n:o 3401 suoritetuista tutkimuksista. Geological Survey of Finland, Archive report, M06/3231/-84/2/10, 4 p.

Makkonen, H., 1992. 1.9 Ga tholeiittinen magmatismi ja siihen liittyvä Ni-Cu –malminmuodostus Juvan alueella, Kaakkois-Suomessa. Unpublished licentiate thesis, University of Oulu, Finland, 200 p.

Makkonen, H.V., 1996. 1.9 Ga tholeiitic magmatism and related Ni-Cu deposition in the Juva area, SE Finland. Geological Survey of Finland, Bulletin 386, 101 p.

Makkonen, H.V., 2005. Intrusion model for Svecofennian (1.9 Ga) mafic-ultramafic intrusions in Finland. In: Autio, S. (ed.) Current Research 2003-2004. Geological Survey of Finland. Special Paper 38, 11–14.

Makkonen, H. & Mäkinen J., 2003. Litogeokemia nikkelimalmien etsinnässä. In: Salminen, R. (ed.) Kuudennet geokemian päivät 12.-13.2.2003, Tiivistelmät, Vuorimiesyhdistys, Sarja B 80, 31–39.

Makkonen, H., Kontoniemi, O., Lempiäinen, R., Lestinen, P., Mursu, J. & Mäkinen, J., 2003. Raahe-Laatokka-vyöhyke, nikkelin ja kullan etsintä-hankkeen (2108001) toiminta vuosina 1999-2003. Geological Survey of Finland, Archive report, M 10.4/2003/5/10, 90 p.

Makkonen, H., Mäkinen, J. & Kontoniemi, O., 2007. Geochemical discrimination between barren and mineralized intrusions in the Svecofennian (1.9 Ga) Kotalahti Nickel Belt, Finland. Ore Geological Reviews, doi:10.1016/j.oregeorev.2006.05.011.

Mungall, J.E., 2007. Crustal contamination of picritic magmas during transport through dikes: the Expo Intrusive Suite, Cape Smith Fold Belt, New Quebec. Journal of Petrology 48, 1021–1039.

Mutanen, T. & Huhma, H., 2003. The 3.5 Ga Siurua trondhjemite gneiss in the Archaean Pudasjärvi Granulite Belt, northern Finland. Bulletin of the Geological Society of Finland 75, 55–68.

Nironen, M., 1997. The Svecofennian Orogen: a tectonic model. Precambrian Research 86, 21–44.

Nironen, M. & Front, K., 1992. The 1.88 Ga old Mäntylä complex, central Finland: emplacement and deformation of mafic to felsic plutonic rocks and associated Mo mineralisation. Bulletin of the Geological Society of Finland 64, 75–90.

O'Brien, H., Huhma, H. & Sorjonen-Ward, P., 1993. Petrogenesis of the late Archaean Hattu schist belt, Ilomantsi, eastern Finland: Geochemistry and Sr, Nd isotopic composition. In: Nurmi, P. and Sorjonen-Ward, P. (eds.) Geological development, gold mineralisation and exploration methods in the late Archaean Hattu schist belt, Ilomantsi, eastern Finland. Geological Survey of Finland Special Paper 17, 145–184.

Pääjärvi, A., 2000. Rautalampi and Karttula. Explanation to the Geological map of Finland 1: 100 000, pre-Quaternary rocks, sheets 3223 and 3224, Geological Survey of Finland, 81 p. (in Finnish with English summary).

Papunen, H., 2003. Ni-Cu sulfide deposits in mafic-ultramafic orogenic intrusions - examples from the Svecofennian areas, Finland. In: Eliopoulos, D. G et al. (eds.) Mineral exploration and sustainable development. Proceedings of the Seventh Biennial SGA Meeting, Athens, Greece, 24-28 August 2003, Vol. 1. Millpress, Rotterdam, pp. 551–554.

Papunen, H., & Koskinen, J., 1985. Geology of the Kotalahti nickel-copper ore. In: Papunen, H., & Gorbunov, G. I. (eds.) Nickel-copper deposits of the Baltic Shield and Scandinavian Caledonides. Geological Survey of Finland, Bulletin 333, 228–240.

Patchett, J. & Kouvo, O., 1986. Origin of continental crust of 1.9-1.7 Ga age: Nd isotopes and U-Pb zircon ages in the Svecokarelian terrain of south Finland. Contributions to Mineralogy and Petrology 92, 1–12.

Pearce, J.A., 1996. A user's guide to basalt discrimination diagrams. In: Wyman, D.A. (ed.) Trace element geochemistry of volcanic rocks: applications for massive sulphide exploration. Geological association of Canada, Short Course Notes 12, 79–113.

Peltonen, P., 1990. Metamorphic olivine in picritic metavolcanics from southern Finland. Bulletin of the Geological Society of Finland 62, 99–114.

Peltonen, P., 1995a. Magma-country rock interaction and the genesis of Ni-Cu deposits in the Vammala Nickel Belt, SW Finland. Mineralogy and Petrology 52, 1–24.

Peltonen, P., 1995b. Petrogenesis of ultramafic rocks in the Vammala Nickel Belt: implications for crustal evolution of the early Proterozoic Svecofennian arc terrane. Lithos 34, 253–274.

Peltonen, P., 2005. Mafic-Ultramafic Intrusions of the Svecofennian Orogen. In: Lehtinen, M., Nurmi, P.A. and Rämö, O.T. (eds.) Precambrian geology of Finland – Key to the evolution of the Fennoscandian Shield. Developments in Precambrian Geology 14, Elsevier, Amsterdam, pp. 413–447.

Peltonen, P., Kontinen, A. & Huhma, H., 1996. Petrology and geochemistry of metabasalts from the 1.95 Ga Jormua ophiolite, northeastern Finland. Journal of Petrology 37, 1359–1383.

Pipping, F., 1972. Viitasaari. Explanation to the Geological map of Finland 1: 100 000, pre-Quaternary rocks, sheet 3311, Geological Survey of Finland, 23 p. (in Finnish with English summary).

Puustinen, K., Saltikoff, B. & Tontti, M., 1995. Distribution and metallogenic types of nickel deposits in Finland. Geological Survey of Finland. Report of Investigations 132, 38 p.

Rämö, O. T., Vaasjoki, M., Mänttäri, I., Elliott, B. A. & Nironen, M., 2001. Petrogenesis of the post-kinematic magmatism of the Central Finland Granitoid Complex I; Radiogenic isotope constraints and implications for crustal evolution. Journal of Petrology 42, 1971–1993.

Rautiainen, I., Hagel-Brunnström, M.-L., Heiskanen, L. & Kallio, E., 1996. Production oriented method for the determination of rare earth and other trace elements in rocks by ICP-MS. In: Nickel, H. and Broekaert, J. A. C. (eds.) XXIX Colloquium spectroscopicum internationale, Leipzig, Germany, August 27-September 1, 1995. Fresenius' Journal of Analytical Chemistry 355, 393–396.

Ruotoistenmäki, T., 1996. A schematic model of the plate tectonic evolution of Finnish bedrock. Geological Survey of Finland, Report of Investigations 133, 23 p.

Sun, S.S., McDonough, W.F., 1989. Chemical and isotopic systematics of oceanic basalts; implications for mantle composition and processes. In: Saunders, A.D., Norry, M.J. (eds.) Magmatism in the Ocean Basin. Geological Society, Special Publication 42, 313–345.

Tuisku, P. & Makkonen, H.V., 1999. Spinel-bearing symplectites in Palaeoproterozoic ultramafic rocks from two different geological settings in Finland: thermobarometric and tectonic implications. GFF 121, 293–300.

Viluksela, A., 1988. Rantasalmen ja Parikkalan-Punkaharjun vulkaniittien petrografia, geokemia ja tektonomagmaattinen luonne. M.Sc. Thesis, University of Helsinki, Finland, 96 p.

Ward, P., 1987. Early Proterozoic deposition and deformation at the Karelian craton margin in southeastern Finland. Precambrian Research 35, 71–93.

Wasserburg, G.J., Jacobsen, S.B., DePaolo, D.J., McCulloch, M.T. & Wen, T., 1981. Precise determination on Sm/Nd ratios, Sm and Nd isotopic abundances in standard solutions. Geochimica et Cosmochimica Acta 45, 2311–2323.

Wilson, M., 1993. Igneous Petrogenesis. Chapman & Hall, London, 466 p.

Appendix 1. Sm-Nd data for Svecofennian metapicrites/metabasalts and mafic-ultramafic intrusions.

Sample/ anal#	Location	Rock type/ mineral	Sm ppm	Nd ppm	$^{147}Sm/^{144}Nd$ (+-0.4%)	$^{143}Nd/^{144}Nd$	2σm	T (Ma)	ε(T) (+-0.4)	map	Northing	Easting	Reference
Previously unpublished data:													
Rantasalmi metalavas:													
RAS-2	Rantasalmi	tholeitic basalt	3.32	11.75	0.1706	0.512437	0.000010	1900	2.4	3233	6881820	3551760	Kousa
RAS-5.1	Rantasalmi	tholeitic basalt	1.85	6.39	0.1751								Kousa
RAS-5.1#2	Rantasalmi	tholeitic basalt	1.89	6.50	0.1753	0.512552	0.000011	1900	3.5	3233	6881530	3550890	Kousa
RAS-10.5	Rantasalmi	tholeitic basalt	4.43	16.88	0.1586	0.512307	0.000010	1900	2.8	3233	6879080	3550860	Kousa
RAS-1.1	Rantasalmi	picrite	3.08	11.15	0.1670	0.512439	0.000013	1900	3.3	3233	6881820	3551820	Kousa
RAS-1.1#2	Rantasalmi	picrite	3.09	11.19	0.1667	0.512436	0.000011	1900	3.3				Kousa
RAS-6.2	Rantasalmi	picrite	1.31	4.33	0.1832	0.512656	0.000015	1900	3.6	3233	6881270	3550980	Kousa
RAS-6.2#2	Rantasalmi	picrite	1.31	4.33	0.1824	0.512647	0.000020	1900	3.6				Kousa
RAS-15	Rantasalmi	picrite	2.35	8.36	0.1698								Kousa
RAS-15#2	Rantasalmi	picrite	2.31	8.22	0.1699	0.512495	0.000010	1900	3.7	3233	6881800	3548050	Kousa
RAS-6	Rantasalmi	picrite	1.77	6.08	0.1764	0.512625	0.000045	1900	(4.7±1)				Kousa
Vammala metapicrites:													
TY-179/125.50-127.50 m	Stormi	cortlandite	1.60	4.97	0.1939	0.512785	0.000020	1900	3.5	212107	6803250	2448100	Peltonen
TY-179/125.50-127.50#2	Stormi	cortlandite	1.61	5.02	0.1942	0.512748	0.000017	1900	2.7	212107	6803250	2448100	Peltonen
TY-193/31.8-32.8 m	Uusiniitty	cortlandite	3.11	13.81	0.1360	0.512055	0.000013	1900	3.4	212107	6801920	2448040	Peltonen
TY-193/31.8-32.8#2	Uusiniitty	cortlandite	3.12	13.84	0.1363	0.512056	0.000017	1900	3.3	212107	6801920	2448040	Peltonen
VM/KML-1/24.0-25.0 m	Komeronlahti	cortlandite	2.31	11.08	0.1262	0.511847	0.000017	1900	1.7	212107	6803580	2445000	Peltonen
Vammala intrusions:													
TY-179-160.0-162.0 m	Stormi	peridotite	0.48	1.79	0.1617	0.512178	0.000018	1880	-0.6	212107	6803250	2448100	Peltonen
TY-179/160.0-162.0#2	Stormi	peridotite	0.48	1.77	0.1638	0.512223	0.000020	1880	-0.2	212107	6803250	2448100	Peltonen
VM/EJ-17/88.60-89.60 m	Ekojoki	peridotite	0.52	2.22	0.1410	0.511951	0.000024	1880	-0.0	212107	6803840	2446840	Peltonen
MHJ/MR-2/77.0-80.0 m	Murto	peridotite	0.76	3.35	0.1364	0.511911	0.000015	1880	0.3	212109	6827180	2444900	Peltonen
VM/SM-1/47.0-48.0 m	Sittamäki	pyroxenite	1.67	7.14	0.1411	0.511963	0.000012	1880	0.2	212105	6811240	2436540	Peltonen
Hyvinkää intrusion:													
R301 178.8	Hyvinkää	pyroxenite	1.94	6.72	0.1750	0.512480	0.000013	1873	2.1				Raitala
39-RTR	Hyvinkää	ultramafite	1.65	7.95	0.1258	0.511904	0.000010	1873	2.7				Raitala
17-RTR	Hyvinkää	ultramafite	0.28	1.00	0.1691	0.512471	0.000023	1873	3.3				Raitala
157.B-RTR	Hyvinkää	gabbro	3.60	14.96	0.1456	0.512131	0.000011	1873	2.3				Raitala
S108.17-RTR	Hyvinkää	gabbro	7.83	34.42	0.1374	0.512043	0.000010	1873	2.6				Raitala
Other intrusions:													
LA-5	Laukunkangas	gabbro	6.38	31.24	0.1235	0.511762	0.000010	1880	0.5	4211	6882700	4435000	Grundström
LA-5 plag	Laukunkangas	plagioclase	0.35	3.27	0.0642	0.511040	0.000013	1880	0.7				Grundström
A1238 (=14-1A-PJL-86)	Kärki Porrasniemi	pyroxenite	1.78	6.48	0.1664	0.512272	0.000012	1880	0.1	213403	6792000	2549000	Lamberg
A1239 (=2-PPL-88)	Kytö Porrasniemi	gabbro	1.49	6.40	0.1405	0.511957	0.000014	1880	0.2	213403	6792180	2548780	Lamberg
A1239px	Kytö Porrasniemi	pyroxene	0.56	2.14	0.1573	0.512148	0.000013	1880	-0.1				Lamberg
A1239pl	Kytö Porrasniemi	plagioclase	0.15	1.68	0.0533	0.510891	0.000015	1880	0.5				Lamberg

A1230wr#2 (P/HY-14/169.0-172.0)	Hyvelä	norite	4.65	23.70	0.1187	0.511684	0.000010	1880	0.2	1143 03	6826070	1543720	Peltonen
A1230px	Hyvelä	pyroxene	1.41	7.00	0.1219	0.511717	0.000010	1880	0.0				Peltonen
A1230px#2	Hyvelä	pyroxene	1.28	6.26	0.1234	0.511735	0.000010	1880	0.0				Peltonen
A1230pl	Hyvelä	plagioclase	0.25	2.96	0.0505	0.510875	0.000010	1880	0.8				Peltonen
A1230pl#2	Hyvelä	plagioclase	0.24	2.99	0.0493	0.510842	0.000014	1880	0.5				Peltonen
A884#2	Kesusmaa Parikkala	gabbro	6.84	34.68	0.1192	0.511797	0.000010	1886	2.3	412407	6835200	4484640	Nykänen
A884#1	Kesusmaa Parikkala	gabbro	6.96	35.45	0.1187	0.511782	0.000010	1886	2.1	412407	6835200	4484640	Nykänen

Published data on intrusions and ultramafic volcanics:

Sample/ anal#	Location	Rock type/ mineral	Sm ppm	Nd ppm	$^{147}Sm/^{144}Nd$ (+-0.4%)	$^{143}Nd/^{144}Nd$	2σm	T (Ma)	ε(T) (+-0.4)	map	Northing	Easting	Reference
A542	Laukunkangas	norite	6.39	31.55	0.1224	0.511729	0.000020	1880	0.1	4211	6882700	4435000	Huhma 1986
S	Salittu	peridotite/ picrite	2.44	9.38	0.1571	0.512307	0.000032	1900	3.2	2023	6688000	2480000	Huhma 1986
A277	Soukkio	gabbro/apatite	142.00	719.00	0.1193	0.511807	0.000030	1870	2.3	2044	6731450	2566430	Huhma 1986
A380	Ylivieska	gabbro	2.05	6.74	0.1844	0.512617	0.000017	1883	2.5	243107	7108620	2521750	Patchett & Kouvo 1986
A584	Hyvinkää	gabbro	2.65	11.19	0.1430	0.512113	0.000015	1880	2.7	204402	6726070	2543380	Patchett & Kouvo 1986
A684	Varissaari	gabbro	11.78	56.21	0.1267	0.511836	0.000021	1885	1.2	212407	6834000	2483000	Patchett & Kouvo 1986
A794	Skåldö	gabbro	3.39	12.72	0.1610	0.512200	0.000018	1885	0.0	201303	6644520	2469700	Patchett & Kouvo 1986
A877	Svartgrund	gabbro	7.30	37.29	0.1183	0.511680	0.000013	1891	0.3	101109	6645020	1446410	Patchett & Kouvo 1986
A568b	Kalanti	gabbro	2.98	14.04	0.1285	0.511955	0.000015	1878	3.1	113107	6747770	1525790	Patchett & Kouvo 1986
R5-53.4	Perämaa	gabbronorite	4.63	20.87	0.1342	0.511892	0.00001	1875	0.4				Rämö et al 2001
OTR-83-16	Perämaa	gabbro	10.68	49.82	0.1296	0.511793	0.000015	1875	-0.4	123410	6891640	1570340	Rämö et al 2001
126-BAE-96	Kälä	gabbro	15.34	72.04	0.1286	0.511775	0.00001	1875	-0.5	321301	6862170	3468750	Rämö et al 2001
Juva ultramafics (Makkonen 1996):													
R361/170.05	Juva	peridotite (Kotalahti type)	3.37	15.82	0.1289	0.511823	0.000010	1880	0.4	323111	6875550	3533800	Makkonen 1996
R344/177.10	Juva	peridotite (Kotalahti type)	0.56	3.12	0.1091	0.511609	0.000014	1880	1.0	314405	6841235	3551030	Makkonen 1996
R374/142.35	Juva	peridotite (Vammala type)	0.89	2.62	0.2058	0.512825	0.000016	1880	1.4	323110	6863095	3530550	Makkonen 1996
R307/61.50	Juva	peridotite (Vammala type)	0.68	3.01	0.1374	0.511968	0.000013	1880	1.2	314402	6840225	3542750	Makkonen 1996
RF/87/1120 (JV-68/13/54.25)	Juva	peridotite (Vammala type)	1.92	6.71	0.1733	0.512472	0.000010	1880	2.4	323110	6860200	3532210	Makkonen 1996
R366/56.70	Rantala	picrite	1.20	4.60	0.1574	0.512252	0.000028	1900	2.0	323111	6872920	3535156	Makkonen 1996
RF/87/682 (R303/84.1)	Rietsalo	gabbro	4.27	20.89	0.1235	0.511816	0.000010	1880	1.6	314402	6849055	3542670	Makkonen 1996

The previously unpublished data above have been analyzed at GTK during nineties using standard methods, sample provided by the geologist in reference.